CGRP neurons and the neural circuitry underlying conditioned taste aversion

Jane Yuhsuan Chen

A dissertation

Submitted in partial fulfillment of the

Requirements for the degree of

Doctor of Philosophy

University of Washington

2019

Reading Committee:

Richard Palmiter, Chair

Larry Zweifel

Sheri Mizumori

Program Authorized to Offer Degree:

Neuroscience

University of Washington

Abstract

CGRP neurons and the neural circuitry underlying conditioned taste aversion

Jane Yuhsuan Chen

Chair of the Supervisory Committee:

Richard Palmiter

Department of Biochemistry

Food aversions develop when the taste of a novel food is associated with sickness, which often occurs after food poisoning or chemotherapy treatment. This phenomenon, known as conditioned taste aversion (CTA), protects animals against repeated self-administration of potentially toxic foods. Despite its importance as a basic survival mechanism, the neural basis of CTA is poorly understood. In order to form a CTA, it is postulated that taste and malaise information converge which results in formation of a long-term memory. A population of neurons in the hindbrain that express calcitonin gene-related peptide (CGRP) has been shown to mediate malaise. Pairing a novel food with activation of CGRP neurons in the parabrachial nucleus (PBN) is sufficient to establish a CTA. Additionally, silencing CGRP neurons can abolish CTA learning. The purpose of this thesis is to delineate the role of CGRP neurons and their downstream projections in the acquisition and expression of CTA. Using in vivo calcium imaging, we show that CGRP neurons are reactivated by the conditioned taste following CTA.

Additionally, CGRP neurons undergo plasticity following CTA and inactivation of genes involved in memory consolidation prevents establishment of a strong CTA. Photoactivation of projections from CGRP neurons in either the central nucleus of the amygdala (CeA) or the bed nucleus of the stria terminalis (BNST) can also induce robust CTA. Activation of CGRP receptor-expressing neurons in the CeA is sufficient to suppress feeding but it does not result in a CTA. Together, these findings show that CGRP neurons not only play a key role for learning food aversions and also contribute to the maintenance and expression of these memories. Future studies that identify additional gene markers in the CeA and BNST will further our understanding of downstream neurons involved in CTA.

Table of Contents

Introduction

Animals innately prefer tastes accompanying calorically rich foods (sweet, fatty) and avoid tastes associated with potentially spoiled or toxic foods (sour, bitter). In addition, animals possess learning mechanisms to modify their feeding behavior through experience. If ingestion of a novel food is followed by gastrointestinal malaise, animals will avoid consuming the same food again in the future. This phenomenon, known as conditioned taste aversion (CTA), is a powerful learning paradigm that protects animals against repeated self-administration of toxic food and ultimately guides ingestive behavior. Not surprisingly, CTA has been demonstrated in many organisms including reptiles (Paradis and Cabanac, 2004; Terrick et al., 1995; Ward-Fear et al., 2016), amphibians (Mikulka et al., 1981), birds (Brett et al., 1976; Martin and Lett, 1985; Wilcoxon et al., 1971), and mammals (Fox et al., 1990; Garcia et al., 1955; Gustavson et al., 1982; Houpt et al., 1990; Terk and Green, 1980). In humans, CTA can influence food selection in the general population as well as in cancer patients undergoing chemotherapy treatment (Bernstein, 1985; Cannon et al., 1983; Garb and Stunkard, 1974; Logue et al., 1981). The propensity to associate overall food consumption with illness greatly contributes to hypophagia observed during medical conditions such as bacterial infection, anorexia nervosa, as well as cancer and chemotherapy. In the latter case, the adverse side effects of chemotherapy can be so severe that some patients will forego treatment despite the obvious life-threatening consequences (Boakes et al., 1993). Thus, understanding the neural circuitry underlying gustatory and visceral signals provide a foundation for the development of treatments or interventions that can ameliorate the debilitating side effects of chemotherapy.

The goal of this thesis is to contribute to our understanding of how the brain integrates taste and malaise signals to prevent repeated consumption of foods that have previously made one ill. More specifically, this thesis focuses on the role of calcitonin gene-related peptide (CGRP) neurons in the parabrachial nucleus (PBN) in acquisition and expression of a CTA. This introduction describes the defining

features of CTA and studies that have directed our attention to the PBN and CGRP neurons. The results section contains a published manuscript showing that CGRP neurons are involved in both the acquisition and expression of a CTA, with further experiments where I manipulated neurons downstream of CGRP neurons in the central nucleus of the amygdala (CeA) that may be involved in CTA. The last section is a summary of my findings and questions that remain unanswered, along with potential approaches to answering key questions, like identifying genetic markers for neurons in the CeA or BNST that mediate taste aversions.

CTA as a classical conditioning paradigm

Taste aversion learning can be considered a type of classical Pavlovian conditioning, where an association is formed between the taste (conditioned stimulus, CS) and subsequent malaise (unconditioned stimulus, US). In many associative-learning paradigms, temporal contiguity between the CS and US are critical for effective conditioning and this temporal proximity has been used to build models of cellular signaling processes that may underlie plasticity at relevant synapses (Abrams and Kandel, 1988), which then gives rise to formation of a long-term memory. However, CTA is unique in that initial exposure to taste (CS) can occur several hours before the illness (US), suggesting that an engram of the novel food persists long after the initial exposure (Reilly, 2009). In agreement, there is evidence that changes in gene expression and neuronal excitability do occur in response to a novel taste. Elevated Fos levels, an immediate early gene used as a marker for neuronal activity, have been observed in the CeA and insular cortex (IC), both of which have been implicated in taste processing and CTA (Koh et al., 2003), Furthermore, NMDA receptor activity in the IC increases in response to a novel taste and this activity is necessary for CTA (Jimenez and Tapia, 2004; Rosenberg et al., 2016). These changes suggest that the novel taste may produce a learning tag in relevant synapses, which when further activated by a US can then facilitate establishing a long-term memory of CTA.

Central pathways underlying taste and malaise

The central gustatory pathway of rodents underlying taste identity has been well characterized (Gal-Ben-Ari and Rosenblum, 2011; Yamamoto and Ueji, 2011). Briefly, taste receptors on the tongue and soft palate relay taste information to the rostral nucleus of the solitary tract (NTS) via cranial nerves VII, IX, and X. In rodents, taste information is then sent to the medial PBN, where it ascends to forebrain processing areas such as the gustatory thalamus (ventral posterior parvocellular nucleus, VPMpc), and primary gustatory cortex region of the insular cortex (IC). Descending fibers from the IC innervate the basolateral amygdala (BLA), which projects to the CeA (Figure 1).

For the US, visceral information is relayed by the vagus nerve to the caudal NTS, which has extensive projections to the lateral PBN. The PBN has been implicated as the major relay of ascending visceral signals from the NTS to the thalamus, hypothalamus, and amygdala (Critchley and Harrison, 2013). Although the specific neuroanatomical projections mediating nausea are still poorly described, several studies have identified regions activated after systemic injection of lithium chloride (LiCl), which is commonly used to induce malaise. Increased expression of Fos was seen in the NTS, PBN, and CeA (St Andre et al., 2007; Yamamoto et al., 1992). The association of visceral malaise (US) and gustatory (CS) information may occur at multiple places along these pathways. The interconnectivity between many of these

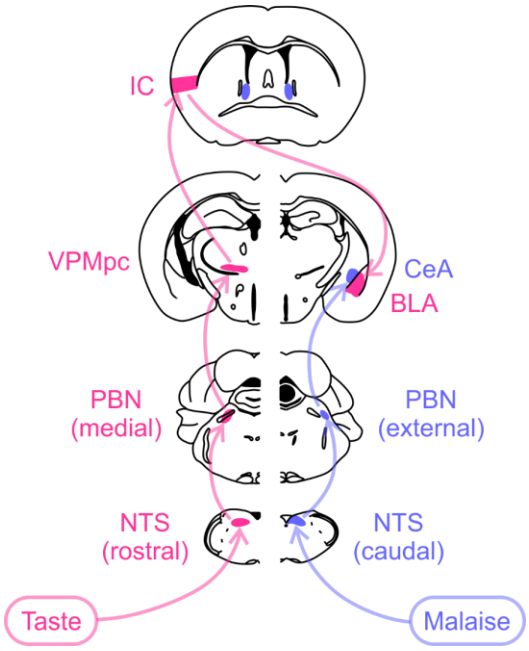

Figure 1. Ascending taste and visceral malaise information follow parallel by separate paths from the cranial nerves to NTS and PBN. From the PBN, taste information is relayed through the VPMpc, IC, then BLA and likely converges with nociceptive visceral signals in the CeA.

regions (Reilly and Bornovalova, 2005, Yamamoto and Ueji, 2011) complicate efforts to identify where the association between taste and illness occurs to produce an aversive taste memory.

CTA and central gustatory lesions

A seminal study by Grill and Norgren in 1978 transected the rat brain at the mesodiencephalic junction, which reduced the functional central gustatory system to the two taste nuclei located in the brainstem, the NTS and PBN. These chronic decerebrate rats failed to acquire a CTA (Grill and Norgren, 1978), suggesting that the NTS and PBN play only a minor role in CTA and sparked the search for forebrain regions responsible for taste-aversion learning. After a decade of research on forebrain areas and CTA, the studies came to one conclusion: lesions of many forebrain regions impair CTA acquisition, but none completely abolish CTA learning (Reilly, 2009). In the hindbrain, lesions of the NTS had little effect on CTA acquisition and expression (Flynn et al., 1991, Grigson, 1997). These studies also observed no impairment in gustatory processing, suggesting that the NTS lesions were incomplete and the gustatory neurons that remained likely contributed to CTA. However, numerous studies have shown that lesions of the PBN disrupt CTA. Specifically, lesions of the medial gustatory PBN result in deficits in taste detection while lesions of the lateral PBN prevent transmission of ascending US signals (Reilly, 1999, Spector et al., 1992). Thus, disruptions of either the CS or US pathway through the PBN prevents learning the association between CS and US.

The parabrachial nucleus and CGRP neurons

The PBN is ideally situated in the dorsolateral pons to receive ascending sensory information from the periphery and relay it to forebrain processing areas. In addition to taste and malaise, the PBN also relays other sensory information such as temperature, olfaction, and almost all nociceptive inputs including pain and itch (Campos et al., 2018, Gauriau and Bernard, 2001, Nakamura and Morrison, 2011). It is

bisected by the superior cerebellar peduncle (scp), a large fiber tract connecting the cerebellum to the brainstem, which separates the medial and lateral regions of the PBN. The waist region comprises neurons within the scp (Fulwiler and Saper, 1984). In addition to its connections within the taste circuitry such as the VPMpc and IC, neurons in the PBN also project to numerous limbic structures, including the CeA, bed nucleus of the stria terminalis (BNST), parasubthalamic nucleus, and lateral hypothalamus. All these forebrain areas, except for the VPMpc, send reciprocal connections back to the PBN (Tokita et al., 2009). The interconnectivity of these regions and the complex role of the PBN has complicated efforts to parse out specific effects of lesion studies without affecting other sensory signaling pathways.

To explore the role of the PBN in CTA, our lab utilizes genetic techniques that allow specific manipulation of defined neuronal populations. We first showed that systemic administration of malaise-inducing factors, like LiCl or LPS, induces Fos in the PBN, which co-localizes in part to neurons that express the calcitonin gene-related peptide (CGRP) (Carter et al., 2013). Direct activation of CGRP neurons in the PBN ($CGRP^{PBN}$ neurons) suppresses feeding and promotes anorexia (Carter et al., 2013). Furthermore, stimulating $CGRP^{PBN}$ neurons is sufficient to induce a CTA and inhibition of these neurons attenuates LiCl-induced CTA (Carter et al., 2015). However, it remained unclear if inhibition of $CGRP^{PBN}$ neurons prevents the acquisition, maintenance, or expression of the taste memory. After CTA acquisition, the conditioned taste induces Fos in the external lateral PBN where CGRP neurons reside (Swank and Bernstein, 1994, Tokita et al., 2007). Since $CGRP^{PBN}$ neurons can also respond to a cue after fear conditioning (Campos et al., 2018), I hypothesized that $CGRP^{PBN}$ neuron activity may also be necessary for the expression of a CTA.

Results

I. Design of CTA paradigm

Although CTA is easily produced in the laboratory, many issues had to be addressed regarding the reproducibility and interpretation of learned-aversion behaviors. First, CTA experiments are commonly designed with one conditioning trial and one test trial. This experimental design is often used since robust and long-lasting CTA is readily acquired when severe visceral malaise is the US (Garcia and Koelling, 1967; Nachman, 1970). However, a one-time activation of specific neuronal populations may not result in a strong CTA, particularly when the paradigm relies on viral-mediated expression of effector molecules in a target population or if stimulation results in a weak CTA that is not readily apparent after a single CS-US pairing. In inactivation studies, a single pairing of CS and US may be insufficient to determine if the inactivation eliminated or simply attenuated CTA learning. Thus, I decided to use multiple conditioning trials. Second, when testing for CTA, a two-bottle procedure (CS versus water) is much more sensitive than a one-bottle test (Dragoin et al., 1971; Elkins, 1973) because it is less impacted by individuals' hydration levels. The mouse can avoid drinking the CS solution by drinking water, which amplifies the magnitude of CTA. Third, it is important to consider the intrinsic properties of both the CS and US and choose them carefully. The previous publication of CTA in our lab used liquid Ensure as the CS (Carter et al., 2015), which has a potent vanilla scent and contains a high amount of glucose polymers (Polycose). However, previous studies have demonstrated the difficulty of obtaining a CTA when Polycose was used as the CS (Bonacchi et al., 2008; Sclafani and Vigorito, 1987), likely due to its high caloric content. With these three issues in mind, I developed a CTA paradigm that addresses these issues. Briefly, mice were acclimated to a restricted drinking water schedule for 3 days so they would be thirsty when exposed to the CS solution. On day 4, water was replaced with a 5% sucrose solution (CS) and followed by an intraperitoneal injection of LiCl (US). This CS-US pairing was repeated

on day 6 and the mice were tested for CTA on day 8 with a two-bottle procedure (sucrose and water). The preference index for sucrose was scored as the amount of sucrose consumed divided by the total fluid consumption. Following this conditioning paradigm, mice develop a robust CTA that persists for >4 weeks (Figure 2A-B). This paradigm was also used to replicate experiments showing that activation of $CGRP^{PBN}$ neurons with both chemogenetics and optogenetics (as described in the next section) is sufficient to establish a CTA (Figure 2).

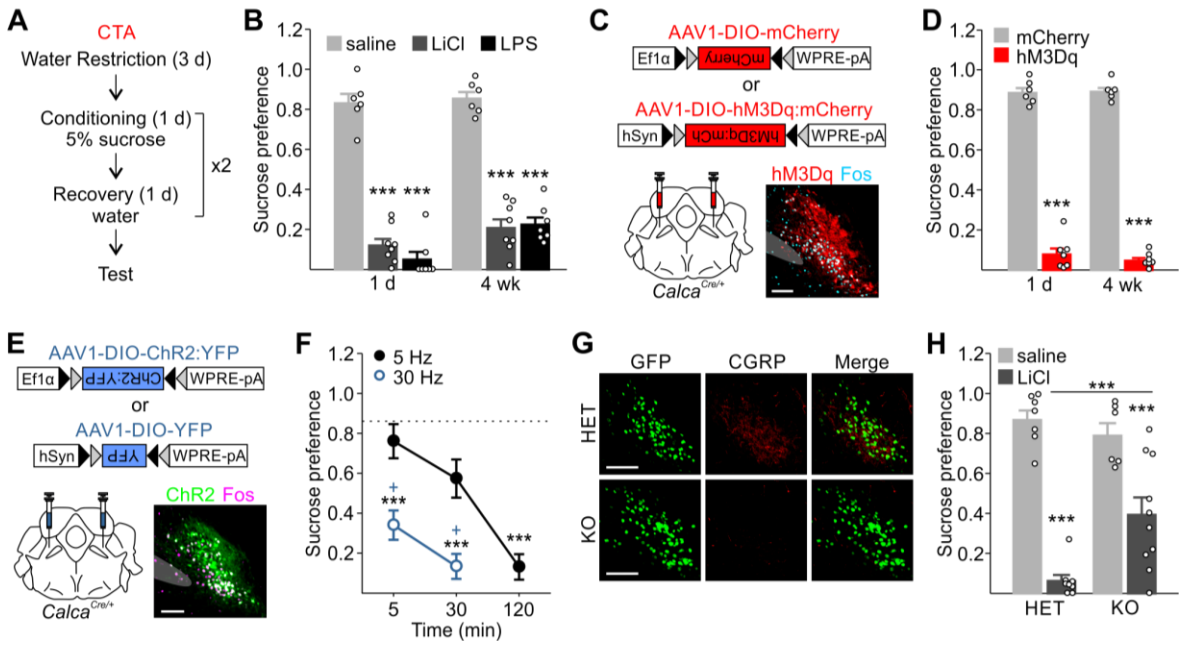

Figure 2. Activation of CGRP neurons induces CTA and involves release of CGRP

(A) CTA conditioning timeline.

(B) Pairing LiCl or LPS with novel sucrose induces CTA that persists for 4 wk (n=6 saline, n=8 LiCl, n=7 LPS; two-way RM ANOVA, treatment: $F_{2,18}$=173.78, P<0.001).

(C) Cre:GFP (green) and CGRP expression (red) in *Calca*$^{Cre/+}$ (HET) and *Calca*$^{Cre/Cre}$ (KO) mice. Scale bar, 100 µm.

(D) CGRP KO mice have attenuated LiCl-induced CTA (HET: n=7 saline, n=8 LiCl; KO: n=6 saline, n=10 LiCl; two-way ANOVA, interaction $F_{1,27}$=8.86, P=0.006).

(E) Bilateral injections of AAV1-DIO-hM3Dq:mCherry or AAV1-DIO-mCherry into the PBN of *Calca*$^{Cre/+}$ mice with representative image of viral expression and induction of Fos in the PBN after CNO administration. Scale bar, 100 µm.

(F) Pairing CNO activation of CGRP^{PBN} neurons with exposure to 5% sucrose causes a robust and long-lasting CTA (n=6 mCherry, n=7 hM3Dq; two-way repeated measures (RM) ANOVA, treatment: $F_{1,5}$=405.84, P<0.001).

(G) Bilateral injections of AAV1-DIO-ChR2:YFP or AAV1-DIO-YFP and fiber optic cannula implants into the PBN of *Calca*$^{Cre/+}$ mice. Representative image shows viral expression and induction of Fos in the PBN after photostimulation. Scale bar, 100 µm.

(H) Robust CTA is acquired with low-frequency, long-duration optogenetic stimulation or high-frequency, short-duration stimulation of CGRP^{PBN} neurons (n=5 for each group; one-way ANOVA, interaction $F_{5,20}$=18.847, P<0.001). Dashed line represents mice injected with YFP and stimulated at 5 or 30 Hz (sucrose preference, 0.86±0.09). Significant differences between groups compared to YFP are denoted by * and significance between 5 and 30 Hz at 5 or 30 min is denoted by +.

Data are reported as mean ± SEM. ***P<0.001.

II. Parabrachial CGRP neurons establish and sustain aversive taste memories

*This section was published with minor reformatting as an article with the same title in *Neuron*. The full citation is as follows:

Chen, J.Y., Campos, C.A., Jarvie, B.C. and Palmiter, R.D. Parabrachial CGRP neurons establish and sustain aversive taste memories (2018) Neuron **4**, 891-899.

Activation of CGRP^{PBN} Neurons Induces CTA and Involves Release of CGRP

To mimic the long-lasting effects of LiCl, *Calca*$^{Cre/+}$ mice were bilaterally injected with AAV1-DIO-hM3Dq:mCherry, an excitatory receptor exclusively activated by clozapine-N-oxide (CNO), into the PBN. Pairing sucrose with an injection of CNO (1 mg/kg) resulted in a robust and long-lasting CTA (Figures 2C and 1D), similar to LiCl- or LPS-induced CTA. LiCl, LPS, and CNO activation of CGRP neurons all have long-lasting effects that persist for >2 h (Carter et al., 2013), but a brief 5-min stimulation of CGRP neurons is also sufficient to induce CTA (Carter et al., 2015). To determine the optimal stimulation parameters for CTA, we used optogenetics with channelrhodopsin, a light-activated cation channel, to vary the stimulus frequency and duration of activation of CGRP^{PBN} neurons. We bilaterally injected AAV1-DIO-ChR2:YFP and implanted fiber optic cannulas over the PBN (Figure 2E). Pairing 5% sucrose with low-frequency, long-duration photostimulation (5 Hz for 120 min) or high-frequency, short-duration stimulation (30 Hz for 30 min) was sufficient to induce a robust CTA, whereas low-frequency, short-duration stimulation (5 Hz for 5 min or 30 min) did not result in CTA (Figure 2F).

To examine the role of CGRP signaling in CTA, we used homozygous *Calca*$^{Cre/Cre}$ mice; the Cre:GFP cassette includes a polyadenylation signal inserted into the 2nd exon, which precludes expression of the downstream exon encoding CGRP. Immunohistochemistry staining for CGRP in the PBN of *Calca*$^{Cre/Cre}$ mice confirmed the absence of CGRP-positive fibers in these knockout (KO) mice (Figure 2G). Pairing

novel sucrose with an injection of LiCl in CGRP KO mice attenuated development of CTA compared to heterozygous (HET) controls (Figure 2H). Interestingly, chemogenetic activation of $CGRP^{PBN}$ neurons expressing hM3Dq in CGRP KO mice still produced a strong CTA (sucrose preference: 0.049±0.00875 in HET and 0.159±0.0942 in KO mice; n=5-6 mice per group, Mann-Whitney rank sum test, U=9, P=0.180). Thus, LiCl-induced CTA requires release of CGRP, but direct activation of $CGRP^{PBN}$ neurons can induce CTA independently of CGRP release.

$CGRP^{PBN}$ Neurons Undergo Plasticity after CTA

As CTA involves learning, we asked whether $CGRP^{PBN}$ neurons undergo plasticity after conditioning. We measured the ratio of AMPA/NMDA receptor currents and frequency of spontaneous excitatory post-synaptic currents (sEPSCs) after CTA. To enhance visualization of CGRP neurons, AAV1-DIO-mCherry was injected into the PBN of $Calca^{Cre/+}$ mice, which co-localized with endogenous Cre:GFP expression (Figures 2A and 2B). Mice were conditioned with 5% sucrose and LiCl injection (as in Figure 2A) and tested for acquisition of CTA 2 d after the last conditioning trial. LiCl-injected (CTA) mice showed a significant increase in AMPA/NMDA ratio compared to control saline-injected mice (Figure 3C and 3D). The increase in AMPA/NMDA ratio was accompanied by a significant increase in the frequency, but not amplitude, of sEPSCs recorded from CTA mice (Figures 3E-G).

We also examined the role of *Arc*, an immediate early gene implicated in memory consolidation (Plath et al., 2006), and *Grin1*, which encodes the essential NR1 subunit of the NMDA receptor and is involved in *Arc* induction, in the development of CTA. To KO *Arc* or *Grin1* selectively in $CGRP^{PBN}$ neurons, we generated a conditional mouse, in which Cre expression at the *Calca* locus is dependent on FLP recombinase ($Calca^{frtCre/+}$, Figure S1). These mice were bred to mice with conditional *Arc* or *Grin 1* alleles (Figures S2A-C) to generate $Calca^{frtCre/+}$:: $Arc^{lox/lox}$ or $Calca^{frtCre/+}$:: $Grin1^{lox/lox}$ (KO) mice. Littermates with the genotype $Calca^{frtCre/+}$::$Grin1^{lox/+}$ or $Calca^{frtCre/+}$::$Arc^{lox/+}$ (HET) were used as controls. Injection of AAV1-

FLP:DsRed and AAV1-DIO-YFP into the PBN allowed expression of Cre and Cre-dependent YFP in $CGRP^{PBN}$ neurons (Figure 3H), which then inactivated the *Arc* or *Grin1* gene in those cells to produce cell-specific KO. Non-CGRP neurons express FLP:DsRed but not Cre-dependent YFP (Figure 3H inset). Expression of Cre resulted in the absence of *Arc* expression in $Arc^{lox/lox}$ mice (unpublished) and abolished NMDAR-mediated currents in $Grin1^{lox/lox}$ mice (Figure S3A).

If either *Arc* or *Grin1* was knocked out in $CGRP^{PBN}$ neurons prior to conditioning, mice were unable to acquire a CTA (Figures 3I-K). Inactivation of *Arc* after CTA was acquired had no effect on the established memory (Figures 3L and 3M). However, if *Grin1* was inactivated after conditioning, the previously learned aversion was attenuated (Figure 3N).

As NMDAR KO may produce changes in excitability, we recorded the firing rate of *Grin1* KO neurons in response to current injection and found that *Grin1* KO neurons were less excitable than controls (Figures S3B and S3C). However, an injection of LiCl decreased food intake in both $Calca^{frtCre/+}$*::Grin1* HET and KO mice (Figure 3O), suggesting that the decrease in excitability does not affect the normal physiological response to LiCl. Together, these results indicate that *Grin1* contributes to both the acquisition and expression of CTA, whereas *Arc* is necessary for acquisition, but not retention or expression, of CTA.

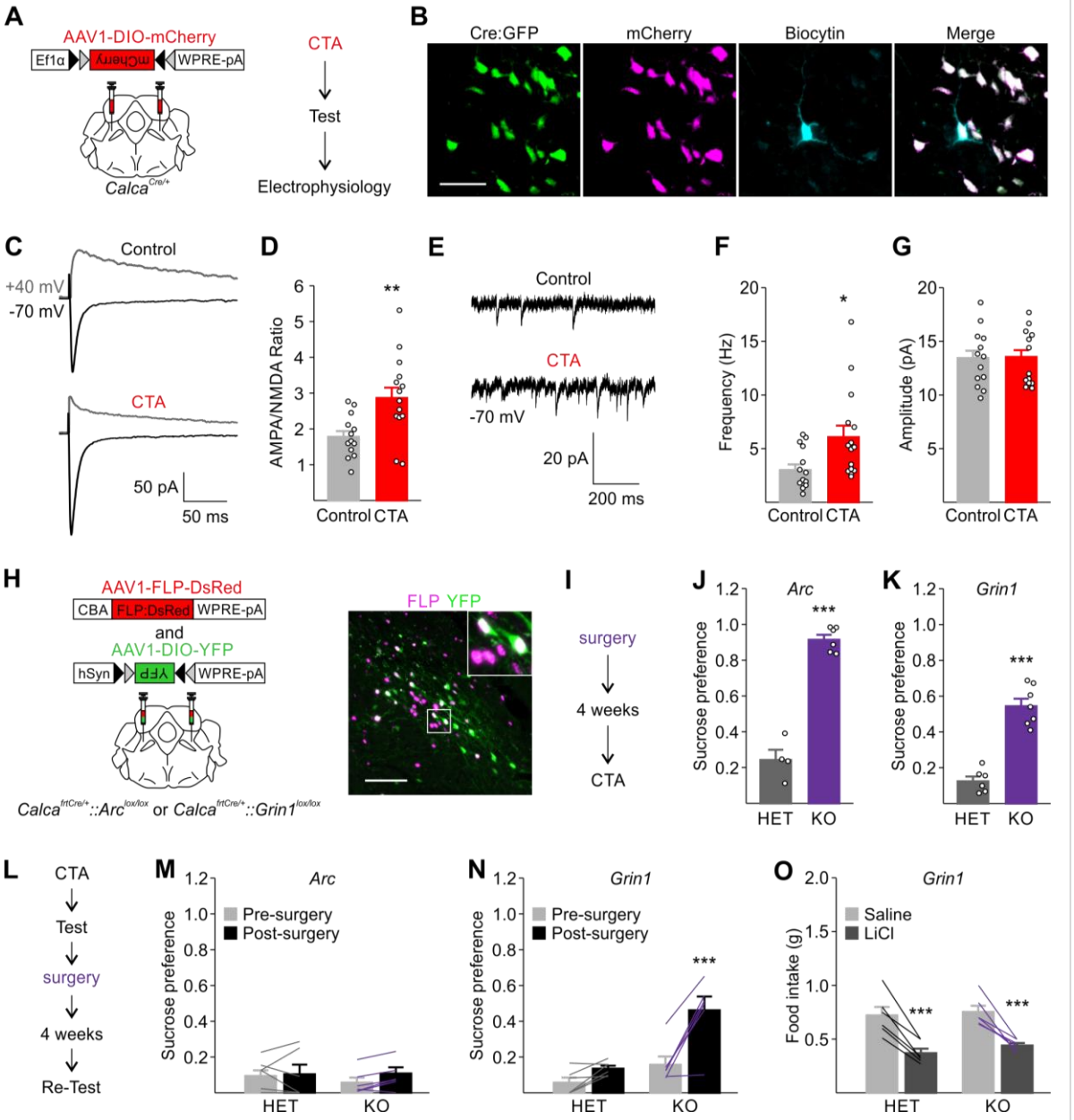

Figure 3. CGRP neurons undergo plasticity after CTA

(A) Bilateral injection of AAV1-DIO-mCherry into PBN of *Calca*$^{Cre/+}$ mice.

(B) Representative image of CGRP neuron co-expressing GFP and mCherry filled with biocytin during recording. Scale bar, 50 µm.

(C) Representative traces of AMPAR- and NMDAR-mediated currents recorded from CGRP neurons of control (top) and CTA (bottom) mice.

(D) Ratios of peak AMPAR- to NMDAR-mediated currents (control: n=13 cells from 4 mice, CTA: n=15 cells from 4 mice, unpaired two-tailed Student's *t* test, $t(26)=-3.153$, $P=0.004$).

(E) Representative traces of sEPSCs from control (top) and CTA (bottom) mice.

(F) Average frequency of sEPSCs (control: n=14 cells from 4 mice, CTA: n=15 cells from 4 mice, Mann-Whitney rank sum test, $U=50$, $P=0.017$).

(G) Average amplitude of sEPSCs (control: n=14 cells from 4 mice, CTA: n=15 cells from 4 mice, unpaired two-tailed Student's *t* test, $t(27)=-0.112$, $P=0.912$).
(H) Bilateral injection of AAV1-FLP:DsRed and AAV1-DIO-YFP into PBN of $Calca^{frtCre/+}::Grin1^{lox/lox}$ or $Calca^{frtCre/+}::Arc^{lox/lox}$ mice results in FLP:DsRed and Cre-dependent YFP expression in the PBN. Scale bar, 100 µm.
(I-K) Inactivation of *Arc* (J) or *Grin1* (K) in $CGRP^{PBN}$ neurons prior to conditioning attenuates LiCl-induced CTA (*Arc*: n=4 HET, n=6 KO, unpaired two-tailed Student's *t* test, $t(8)=-11.701$, $P<0.001$; *Grin1*: n=6 HET, n=7 KO, Mann-Whitney rank sum test, $U=0$, $P=0.001$).
(L-N) Inactivating *Grin1* (N), but not *Arc* (M) after conditioning blocks expression of CTA (n=6 for each group; *Grin1*: two-way RM ANOVA, interactions: $F_{1,10}=10.677$, $P=0.008$; *Arc*: two-way RM ANOVA, interaction: $F_{1,10}=1.142$, $P=0.310$).
(O) Inactivation of *Grin1* does not affect LiCl-induced reduction of food intake. (n=6 in each group, two-way RM ANOVA, treatment: $F_{1,10}=69.781$, $P<0.001$).
Data are reported as mean ± SEM. *$P<0.05$, **$P<0.01$, ***$P\leq0.001$. See also Figures S1, S2, and S3.

$CGRP^{PBN}$ Neurons are Active during Expression of CTA.

$CGRP^{PBN}$ neuron activation can act as the unconditioned stimulus (US) during CTA learning and these neurons undergo synaptic plasticity after CTA. Therefore, we hypothesized that the novel taste (conditioned stimulus, CS) can act as an US after conditioning by reactivating $CGRP^{PBN}$ neurons. To test this hypothesis, mice were injected with AAV1-DIO-GCaMP6m, a fluorescent calcium indicator, and implanted with a gradient-index lens over the PBN to monitor CGRP neuronal activity in awake animals (Figure 4A). After a single conditioning trial with 30-min access to a novel food (vanilla Ensure), mice were given an injection of LPS (50 µg/kg), or saline for controls. Two days later, mice were videotaped during re-exposure to Ensure while changes in fluorescence was recorded with miniature microscope (Inscopix) that allows visualization of calcium activity in individual CGRP-expressing neurons. We observed little change in fluorescence of $CGRP^{PBN}$ neurons when Ensure was not present. In mice that received LPS (CTA), fluorescence increased in virtually all of the neurons after Ensure was presented, which was not observed in control mice that received saline (Figures 4B and 4D). While some changes in fluorescence coincided with head movements (Figures S4A and S4B), there was no significant change in correlation between movement distance and changes in fluorescence after Ensure was presented (Figure 4C, Figures S4A and S4B). In contrast, when control mice approached the Ensure bottle, there

was relatively little change in CGRP-neuron fluorescence (Figure 4B and 4D). The average locomotor activity of CTA mice was less than control mice during re-exposure to Ensure (Figure 4E). Under anesthesia, presentation of a cotton swab dipped in Ensure increased fluorescence of CGRP neurons of CTA mice, but not control mice (Figure 4F), demonstrating that CGRP neurons can be activated by the smell of Ensure in the absence of locomotion. These results reveal that the CS (taste and/or smell of Ensure) can act as an US after conditioning.

To explore the functional role of $CGRP^{PBN}$ neurons in the expression of CTA, we silenced $CGRP^{PBN}$ neurons with tetanus toxin (AAV1-DIO-GFP:TeTx) after establishing a CTA. These mice consumed more Ensure during 7 d of extinction compared to control mice (Figure 4G). Silencing $CGRP^{PBN}$ neurons increased Ensure intake in control mice, so we also examined the effects of transiently inhibiting $CGRP^{PBN}$ neurons during CTA expression. *Calca*$^{Cre/+}$ mice were co-injected with AAV1-DIO-hM3Dq:mCherry and AAV1-DIO-KORD:mCitrine (an inhibitory receptor activated by salvinorin B, SalB), to bidirectionally modulate CGRP neural activity (Figure 4H). Pairing 5% sucrose with activation of $CGRP^{PBN}$ neurons via CNO induced a strong CTA, but inhibition of the neurons with SalB prior to testing attenuated expression of CTA, and this pattern was repeated with subsequent testing (Figure 4I). When CNO and SalB were co-administered, the suppression of food intake caused by activation of $CGRP^{PBN}$ neurons was also attenuated (Figure S5A). In agreement, co-injection of CNO and SalB reduced the number of Fos-positive cells observed in the PBN (Figures S5B and S5C), indicating that SalB effectively inhibits neurons that otherwise would be activated by CNO. These results support the observation that not only are $CGRP^{PBN}$ neurons activated by the CS after learning, but their activity is important for expression of a previously learned CTA.

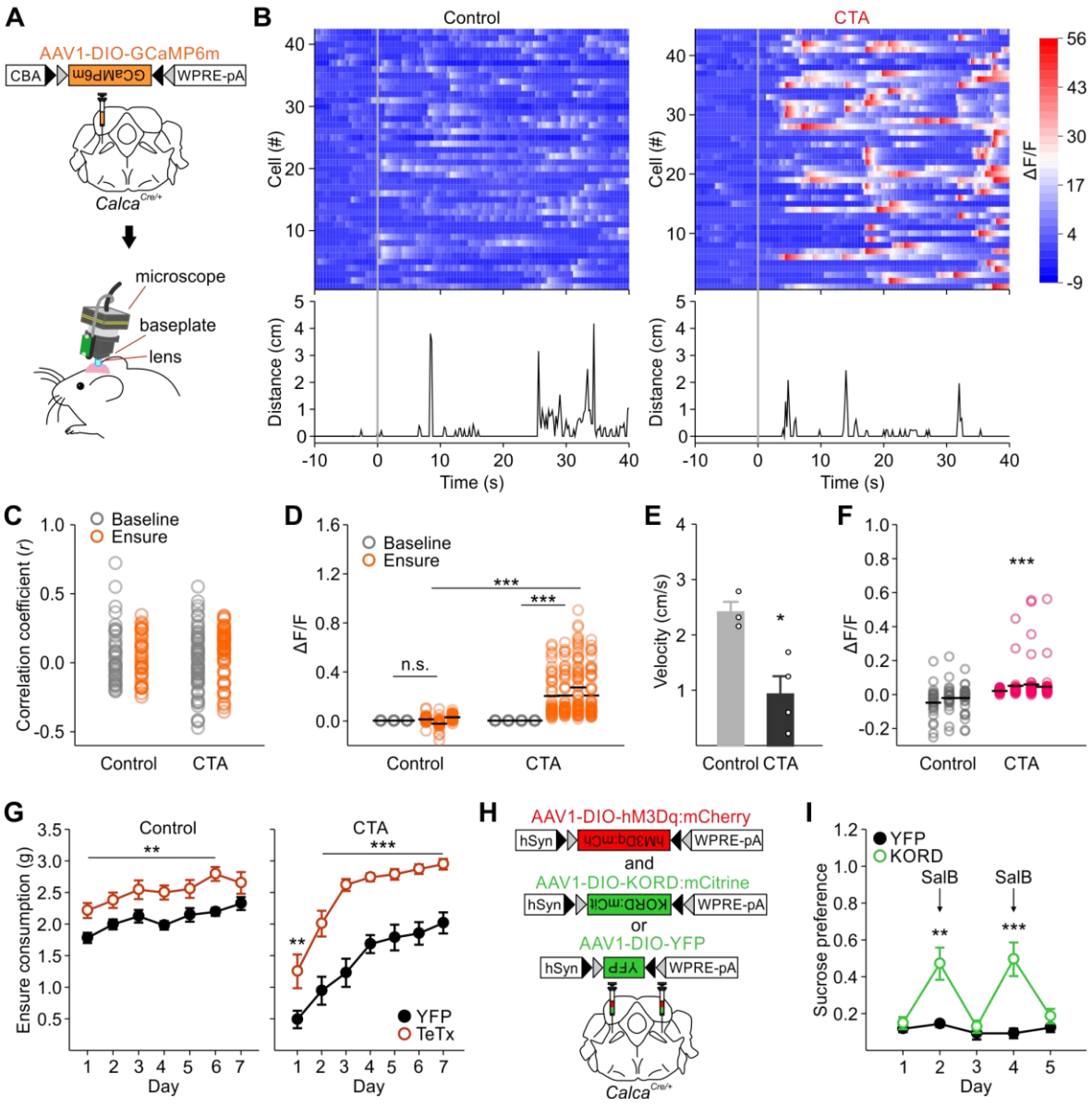

Figure 4. CGRP neurons are active during expression of CTA

(A) Injection of AAV1-DIO-GCaMP6m into the PBN of *Calca*$^{Cre/+}$ mice and diagram of calcium imaging set-up.

(B) Sample responses of CGRP^{PBN} neurons before and after Ensure presentation (top) and corresponding head movements (bottom) of a control (left) and CTA-treated (right) mouse.

(C) Correlation coefficients for the changes in fluorescence of each cell and head movements of mice shown in (B). There was no significant change in correlation coefficients after Ensure was presented (two-way RM ANOVA, time: $F_{1,104}$=2.100, P=0.343).

(D) Responses of CGRP^{PBN} neurons at baseline (30 s) and after Ensure presentation (90 s). Each column represents all cells recorded from the same mouse (control: n=134 neurons from 3 mice, CTA: n=202 neurons from 4 mice). The average population response from each mouse, indicated by the horizontal black line, was used for statistical analysis (two-way RM ANOVA, interaction $F_{1,5}$=83.358, P<0.001).

(E) Average movement velocity of control and CTA mice during re-exposure to Ensure. (control: 3 mice, CTA: 4 mice, unpaired two-tailed Student's t-test, t(5)=3.538, P=0.017).

(F) Responses of CGRP^{PBN} neurons to the smell of Ensure while mice are under anesthesia. Each column represents all cells recorded from the same mouse (control: n=134 neurons from 3 mice, CTA: n=202 neurons from 4 mice). The average population response from each mouse, indicated by the horizontal black line, was used for statistical analysis (unpaired two-tailed Student's t-test, t(5)=-6.299, P=0.001).
(G) Pairing Ensure with injection of LPS results in a strong CTA; pairing novel Ensure with saline does not induce CTA (left), whereas inactivation of CGRP neurons with TeTx after learning attenuates CTA (left) during 7 d of extinction testing (n=10 in each group, two-way RM ANOVA, virus: $F_{1,108}$=32.217, P<0.001). In agreement with previous findings (Campos et al., 2016), TeTx-treated mice consume more Ensure than YFP controls (n=6 in each group, two-way RM ANOVA, virus: $F_{1,60}$=11.554, P=0.007).
(H) Bilateral injection of AAV1-DIO-hM3Dq:mCherry and AAV1-DIO-KORD:mCitrine or AAV1-DIO-YFP into PBN of *Calca*$^{Cre/+}$ mice for bidirectional modulation of CGRP^{PBN} neuron activity.
(I) Pairing CNO activation of CGRP^{PBN} neurons with novel sucrose induces CTA while subsequent inhibition of the same neurons with SalB on days 2 and 4 of testing prevents expression of CTA (n=7 YFP, n=16 KORD, two-way RM ANOVA, interaction: $F_{1,84}$=7.787, P<0.001)
Data are reported as mean ± SEM. **P<0.01, ***P≤0.001. See also Figures S4 and S5.

Stimulation of CGRP^{PBN} Projections Results in CTA

Since CGRP^{PBN} neurons send strong projections to the CeA, BNST, and VPMpc (Figure S6), we investigated the effects of stimulating each of these downstream sites on CTA by injecting AAV1-DIO-ChR2:YFP into the PBN and placing bilateral fiber optic cannulas over each of the target regions (Figure 5A). Pairing stimulation of CGRP^{PBN} projections to the CeA or BNST (30 Hz for 30 min) with 5% sucrose induced CTA and reduced food intake for 1-2 h (Figures 5B and 5C), whereas stimulating the projection to the VPMpc had no effect. These data suggest that there is redundant circuitry involved in CTA learning.

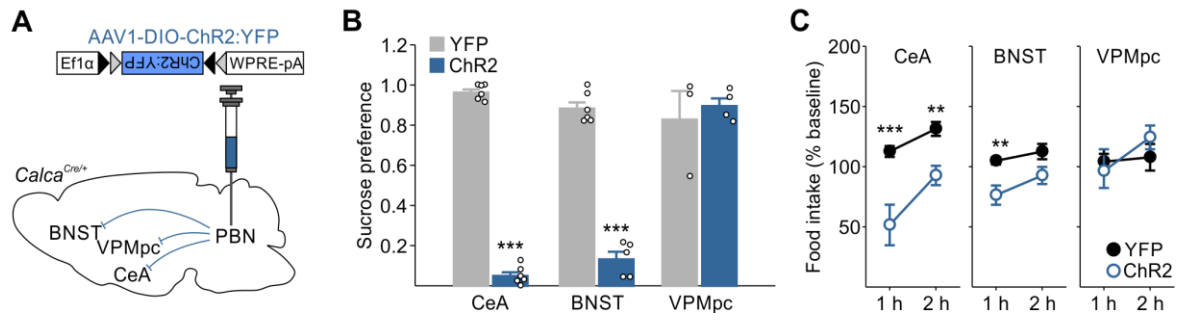

Figure 5. Stimulation of CGRP projections induces CTA
(A) Bilateral injections of AAV1-DIO-ChR2:YFP or AAV1-DIO-YFP into the PBN of *Calca*$^{Cre/+}$ mice with fiber optic cannula implants into the CeA, BNST, or VPMpc.
(B) Pairing stimulation of CGRP^{PBN} projections (30 min at 30 Hz) to the CeA or BNST, but not the VPMpc, with novel sucrose induces CTA (B) (CeA: n=5 YFP, n=6 ChR2, unpaired two-tailed Student's *t* test, $t(10)=37.504$, $P<0.001$; BNST: n=6 YFP, n=5 ChR2, unpaired two-tailed Student's *t* test, $t(9)=15.484$, $P<0.001$; VPMpc: n=3 YFP, n=4 ChR2, unpaired two-tailed Student's *t* test, $t(5)=-0.519$, $P=0.626$).
(C) Photostimulation of axonal projections to CeA and BNST, but not VPMpc, reversibly inhibits food intake) (CeA: n=5 YFP, n=6 ChR2, two-way RM ANOVA, virus: $F_{1,8}=15.142$, $P=0.005$; BNST: n=6 YFP, n=5 ChR2, two-way RM ANOVA, virus: $F_{1,8}=9.489$, $P=0.015$; VPMpc: n=8 YFP, n=8 ChR2, two-way RM ANOVA, virus: $F_{1,28}=0.908$, $P=0.357$).
Data are reported as mean ± SEM. $^{**}P<0.01$, $^{***}P<0.001$. See also Figure S6.

Discussion

We demonstrated that pairing a novel food with either LiCl or LPS is sufficient to generate a robust and long-lasting CTA in which CGRP itself plays a role. Direct chemogenetic or optogenetic activation of CGRP^{PBN} neurons without peripheral visceral malaise is also sufficient to induce CTA. Importantly, we also reveal that CGRP^{PBN} neurons undergo plasticity after learning and that their activity is necessary for expression of CTA. *Grin1* expression within CGRP^{PBN} neurons is necessary for acquisition and expression of CTA, while *Arc* is only necessary for CTA acquisition. Stimulation of CGRP^{PBN} projections to either the CeA or BNST mimics CTA induced by stimulation of CGRP^{PBN} cell bodies. While we suspect that mice develop a conditioned aversion to sucrose or Ensure, our assay only measures consumption; thus, our experiments do not distinguish between taste aversion and avoidance (Dwyer et al., 2017, Garcia and Koelling, 1966).

We observed that CGRP KO mice develop an attenuated CTA, which supports the idea that LiCl activation of CGRP^{PBN} neurons stimulates release of CGRP to facilitate learning the taste aversion. In

agreement, pairing saccharin with an intracerebroventricular administration of CGRP results in a mild CTA (Krahn et al., 1986), indicating that CGRP can participate in development of a CTA. CGRP neurons are glutamatergic (Carter et al., 2013) and they express several other neuropeptides including β-CGRP (unpublished observations), suggesting that CGRP may be one of several signaling molecules that are involved in generating a CTA. In contrast to LiCl-mediated CTA, development of CTA after chemogenetic activation of $CGRP^{PBN}$ neurons was unaffected by loss of CGRP. A likely explanation for this disparity is that direct chemogenetic activation of $CGRP^{PBN}$ neurons is more robust than that achieved by LiCl; hence, release of the other transmitters makes CGRP unnecessary.

Learning to avoid a potentially toxic taste ultimately requires consolidation of a long-term memory. Our finding that $CGRP^{PBN}$ neurons exhibit synaptic plasticity after learning suggests that the PBN is involved in not only CTA acquisition, but also the expression of the learned aversion. Inactivation of *Arc*, an immediate early gene involved in memory consolidation (Plath et al., 2006), prevents establishment of CTA. This indicates a critical role for synaptic plasticity in these neurons during formation of an aversive taste memory. As induction of *Arc* requires NMDA receptor activation (Chen et al., 2017, Steward and Worley, 2001), knocking out NMDA receptors (*Grin1* KO) in $CGRP^{PBN}$ neurons also prevents establishment of a CTA. Interestingly, inactivation of *Grin1* in these neurons after learning attenuated expression of CTA, suggesting that the CS activation of $CGRP^{PBN}$ neurons after learning also requires signaling through NMDA receptors. Furthermore, since *Arc* is only involved in memory consolidation (Nakayama et al., 2015, Ploski et al., 2008), not expression, it follows that inactivation of *Arc* in $CGRP^{PBN}$ neurons after learning has no effect on CTA expression.

We demonstrated that after conditioning, the CS can re-activate $CGRP^{PBN}$ neurons. Transiently inhibiting (KORD with SalB) or permanently silencing (TeTx) these neurons after learning attenuated the expression of a CTA and promotes extinction. Previously, we showed that activation of $CGRP^{PBN}$ neurons reduces food intake (Carter et al., 2013) and is aversive (Han et al., 2015), which indicate that they relay

the US during conditioning. Following the traditional model of Pavlovian conditioning, after an association between the CS and US is formed, the CS acts similar to the US to elicit behavioral responses (Fanselow and Wassum, 2015, Rescorla, 1988). However, the neurocircuitry that allows the CS to mimic the US signal has not been identified. Most models suggest that synaptic plasticity within target neurons where the CS and US signals converge allow the CS to activate the US responsive neurons (Johansen et al., 2011, Maren, 2005, Sah et al., 2008). These experiments provide evidence that after conditioning the CS activates the $CGRP^{PBN}$ neurons, which initially relayed the US signal. In agreement, $CGRP^{PBN}$ neurons also respond to the CS after fear conditioning (Campos et al., 2018). The neural circuitry that allows the CS to activate US-responsive neurons after learning remains to be elucidated.

Taken together, these data reveal a critical role of $CGRP^{PBN}$ neurons in both the acquisition and expression of an aversive taste memory. Furthermore, the frequency and duration of $CGRP^{PBN}$ stimulation influences the strength of the CTA acquired. Consequently, either severe malaise lasting for a short period or weak malaise lasting for an extended time can promote a strong CTA. That latter situation is commonly observed with food poisoning and chemotherapy.

Supplemental Figures

Supplemental Figure S1. Related Figure 2. Generation of *Calca*^{frtCre} Mice

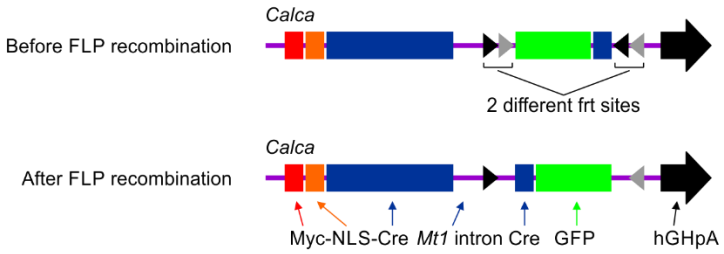

Supplemental Figure 1. Related to Figure 2. Generation of *Calca*^{frtCre} Mice
Diagram showing the Frt-DIO-mnCre:GFP cassette before (top) and after (bottom) FLP-mediated recombination. This cassette was substituted for Cre:GFP in the CalcaCre:GFP construct described previously (Carter et al., 2013). See STAR Methods for details.

Supplemental Figure S2. Related Figure 2. Generation of Conditional *Arc* Mice

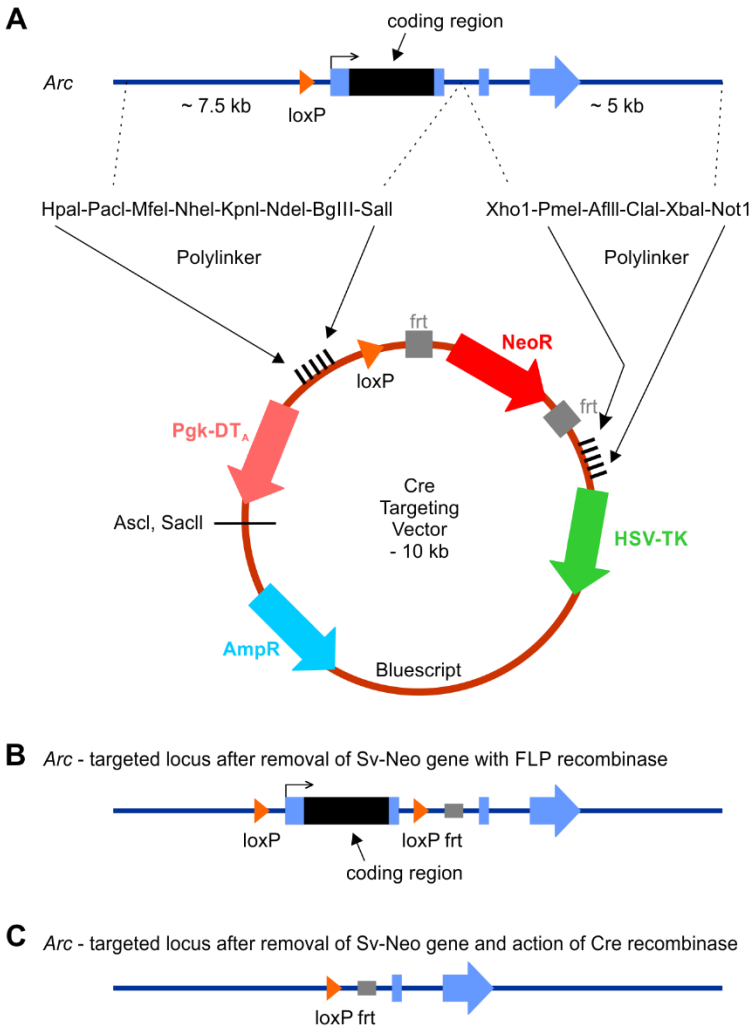

Supplemental Figure 2. Related to Figure 2. Generation of Conditional *Arc* Mice
Diagram showing: the Arc gene with coding region in black and targeting vector (A); loxP sites flanking the coding region (B); and removal of the entire coding region by action of Cre recombinase (C). Some key restriction enzyme sites used for cloning are shown. See STAR Methods for details.

Supplemental Figure S3. Related to Figure 2. *Grin1* KO Decreases Intrinsic Excitability of PBN Neurons

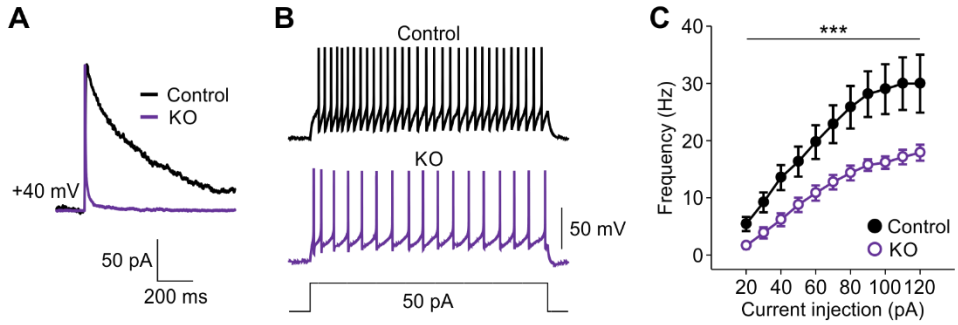

Supplemental Figure 3. Related to Figure 2. *Grin1* KO Decreases Intrinsic Excitability of PBN Neurons

(A) Representative traces of evoked NMDAR EPSCs from control and KO cells. Absence of NMDAR-mediated current was observed in 6/6 KO cells from 2 mice.

(B) Representative traces of action potentials evoked by 2 s current injection in control (top) and KO (bottom) cells.

(C) Action potential frequencies in control and KO cells in response to current injection (control: n=12 cells from 4 mice; KO: n=15 cells from 4 mice, two way RM ANOVA, interaction: $F_{10,250}$=3.732, P<0.001).

Supplemental Figure S4. Related to Figure 3. Calcium Imaging during Re-exposure to Ensure after CTA

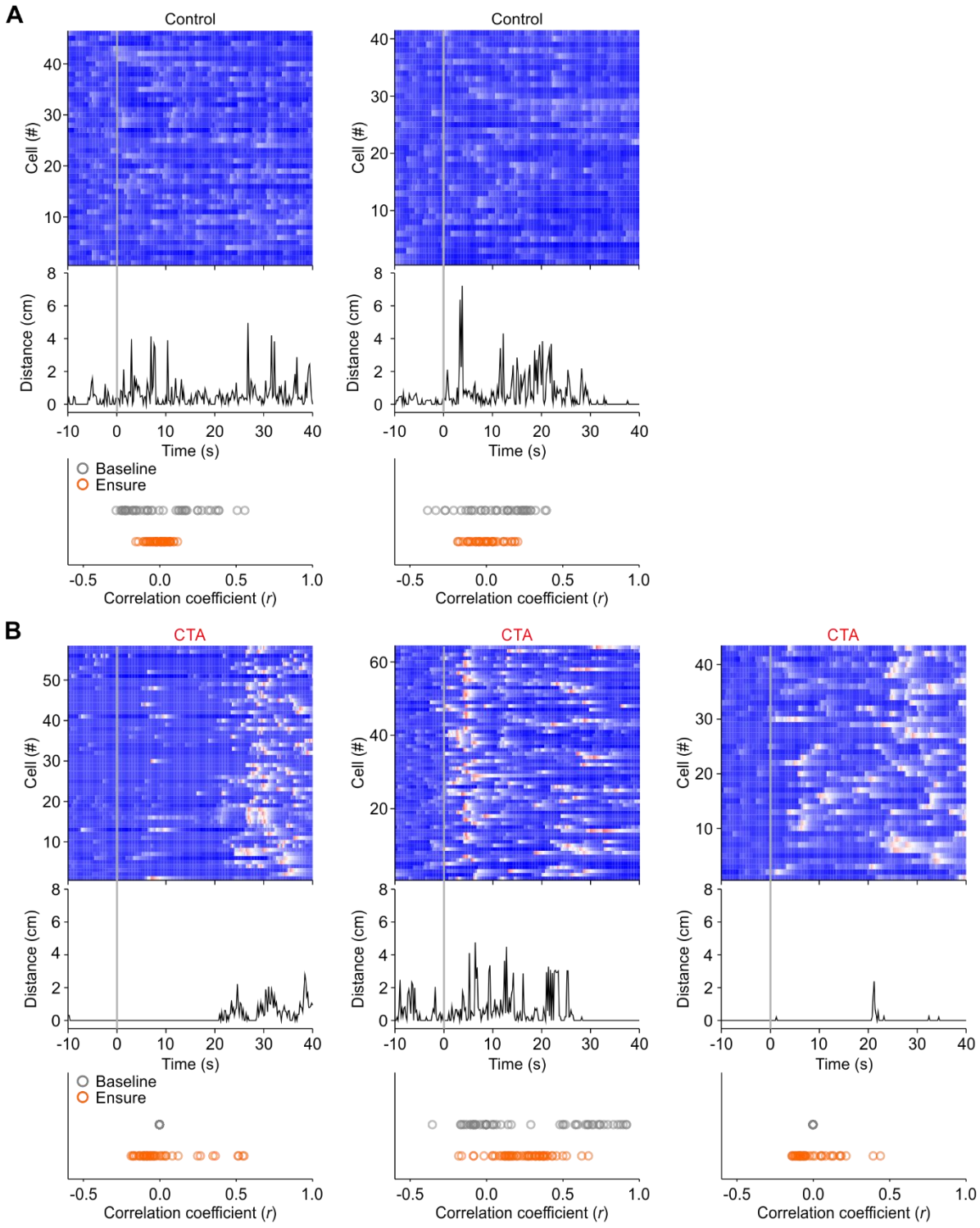

Supplemental Figure 4. Related to Figure 3. Calcium Imaging during Re-exposure to Ensure after CTA
(A-B) Responses of CGRP^{PBN} neurons before and after Ensure presentation (top), corresponding head movements (middle), and correlation coefficients of the change in fluorescence of each cell and head movements of control (A) and CTA (B) mice.

Supplemental Figure S5. Related to Figure 3.Validation of KORD

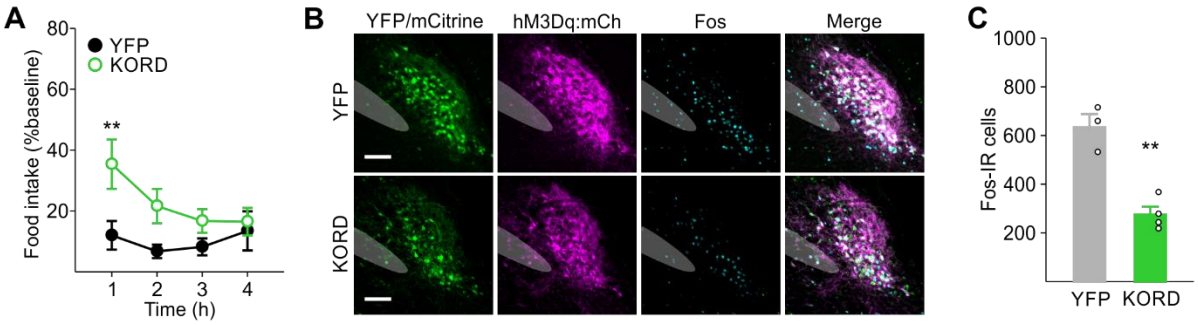

Supplemental Figure 5. Related to Figure 3. Validation of KORD

(A) CNO activation of CGRP^{PBN} neurons suppresses food intake, which was attenuated by co-administration of SalB (n=7 YFP, n=9 KORD, two-way RM ANOVA, interaction: $F_{1,42}$=3.494, P=0.024)

(B) Representative image showing co-expression of hM3Dq:mCherry, KORD:mCitrine or YFP, and Fos in the PBN after co-administration of CNO and SalB. Scale bar, 100 µm.

(C) SalB decreases the amount of Fos induced by CNO activation of CGRP^{PBN} neurons (n=3 YFP, n=4 KORD, unpaired two-tailed Student's t-test, t(5)=6.033, P=0.002).

Supplemental Figure S6. Related to Figure 4. Projections of CGRP^{PBN} Neurons

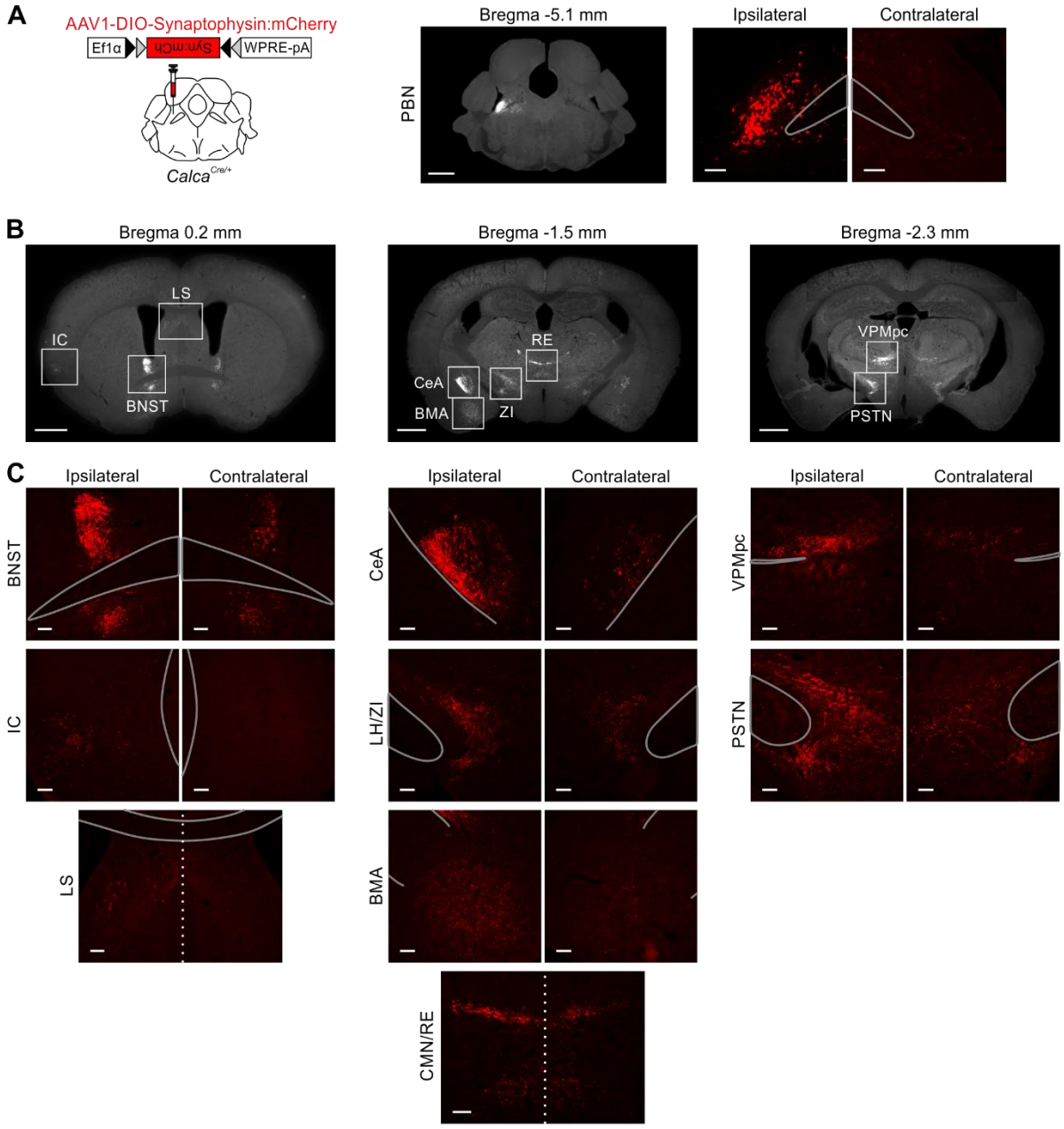

Supplemental Figure 6. Related to Figure 4. Projections of CGRP^{PBN} Neurons

(A) Unilateral injection of AAV1-DIO-Synaptophysin:mCherry into a *Calca*$^{Cre/+}$ mouse (left) results in mCherry expression in the PBN (middle, Scale bar, 1 mm). There are very few projections to the contralateral side of the PBN (right). Scale bar, 100 µm.

(B) Representative images of major projection sites. Scale bar, 1 mm.

(C) Images of regions highlighted in (B) showing projections to both the ipsilateral and contralateral sides relative to the injection site. Scale bar, 100 µm. Dotted line represents midline. BMA, basomedial amygdala; BNST, bed nucleus of stria terminalis; CeA, central nucleus of the amygdala; CMN, central medial thalamus, IC, insular cortex; LH, lateral hypothalamus; LS, lateral septum, PSTN, parasubthalamic nucleus; RE, nucleus of reunions; VPMpc, parvicellular part of ventral posteriomedial thalamus; ZI, zona incerta.

III. Identifying neurons in the CeA involved in CTA

We have shown that photoactivation of $CGRP^{PBN}$ fibers terminating in the CeA suppresses feeding (Carter et al., 2013) and photoactivation of these terminals can substitute for the US in CTA (Figure 5, Chen et al., 2018). Presumably, activation of CeA neurons directly downstream of CGRP neurons will also be sufficient to establish a robust CTA. We previous described a population of neurons in the CeA that express the CGRP receptor (Calcrl) and are monosynaptic targets of CGRP neurons (Han et al., 2015). Activation of these Calcrl neurons can substitute for the US during fear conditioning (Han et al., 2015). Although Calcrl neurons in the CeA are a likely candidate for neurons that could mediate CTA, other neurons could be involved as well. The experiments in this section describe my attempts to identify CeA neurons that when stimulated after consumption of a novel food will result in CTA.

Activation of CGRP receptor-expressing neurons in the CeA

To determine whether Calcrl is a good maker for neurons in the CeA mediating CTA, I tested whether Calcrl neurons can be activated by a common US used to induced malaise. LiCl has been shown to induce Fos expression in the CeA (Yamamoto et al., 1992, Swank and Bernstein, 1994, Hamamura et al., 2000) but it only partially (~50%) colocalizes with Calcrl neurons (Figure 6A). Based on previous studies in the lab using activation of $Calcrl^{CeA}$ neurons as the US during fear conditioning, I tested whether activation of the same neurons can substitute as the US during CTA acquisition. I injected AAV1-DIO-hM3Dq:mCherry or AAV1-DIO-mCherry into CeA of *Calcrl*$^{Cre/+}$ mice, and paired sucrose intake with Calcrl activation by injecting CNO (1 mg/kg) immediately following 30-min access to sucrose. Unlike CNO activation of CGRP neurons, activation of Calcrl neurons in the CeA with CNO did not result in CTA (Figure 6B). As hM3Dq activates the Gq signaling pathway and is dependent on the pharmacokinetics of CNO, it is difficult to control the precise temporal activation and firing rate of neurons with this method.

Thus, I also injected *Calcrl*$^{Cre/+}$ mice with either AAV1-DIO-ChR2:YFP or AAV1-DIO-YFP into the CeA and implanted with bilateral fiber optic fibers for photoactivation. Pairing sucrose with 30-Hz photostimulation also failed to generate a CTA (Figure 6B). However, activation of Calcrl neurons was sufficient to suppress feeding (Figure 6C) and was aversive in a real-time, place-preference (RTPP) test (Figure 6D) in a frequency-dependent manner, similar to what is seen following activation of CGRP neurons in the PBN. Therefore, while Calcrl neurons in the CeA may contribute to anorexia and place avoidance, they do not appear to be involved in CTA acquisition.

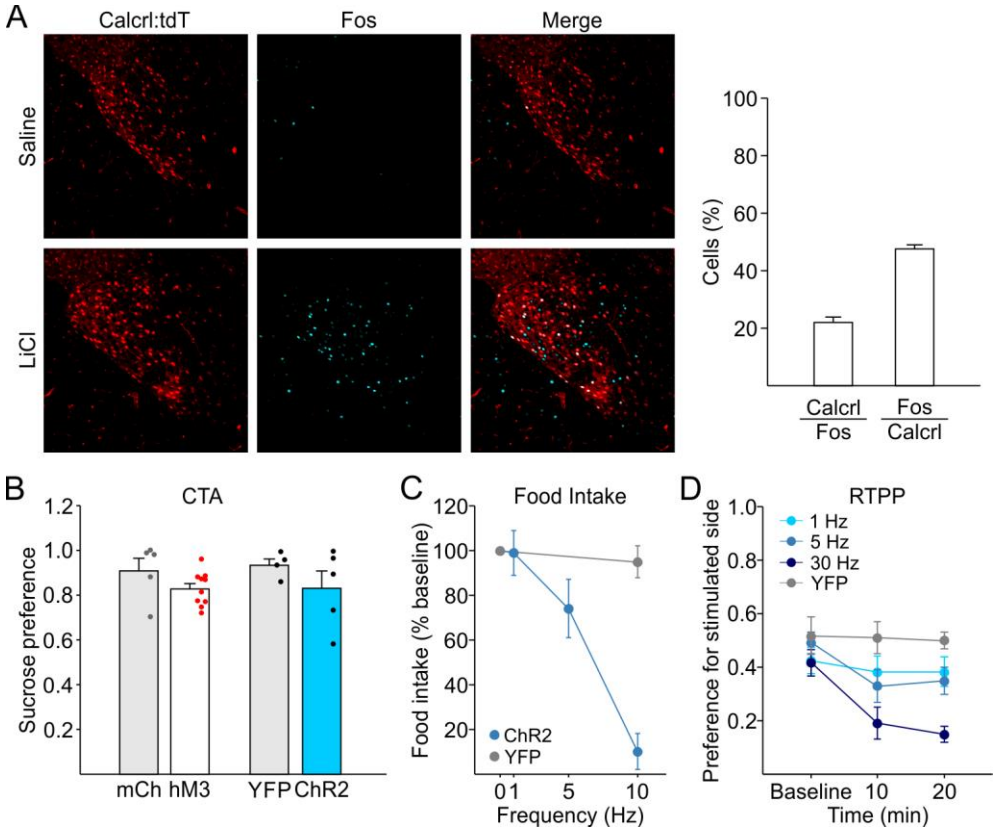

Figure 6. Activation of Calcrl neurons in the CeA does not result in CTA
(A) LiCl induces Fos in Calcrl neurons
(B) Pairing chemogenetic or optogenetic activation of Calcrl neurons with exposure to 5% sucrose does not result in CTA (n=5 mCherry, n=9 hM3Dq, n=4 YFP, n=5 ChR2.
(C) 10 Hz stimulation of Caclrl neurons suppresses food intake
(D) High frequency (30 Hz), but not low (1 and 5 Hz), stimulation is aversive in a RTPP test

Activation of other neurons in the CeA

Based on RiboTag experiments which identify actively translated mRNAs, we know that CGRP neurons also express multiple neuropeptides including neurotensin, pituitary adenylyl cyclase activating peptide (PACAP), tachykinin 1 (substance P), and dynorphin (unpublished data). Thus, our lab has created Cre-driver mouse lines for receptors of each of these neuropeptides, which are likely to be expressed downstream of CGRP neurons in the CeA and other target regions. So far, I injected AAV1-DIO-ChR2:YFP into two of these Cre-driver lines including the receptor for tachykinin 1 (TacR1) and PACAP (Pac1R). None of these mice developed a CTA when activation of these neurons was paired with novel sucrose (Figure 7A). However, activation of either TacR1 or Pac1R neurons with 30-Hz photostimulation effectively suppressed feeding (Figure 7B).

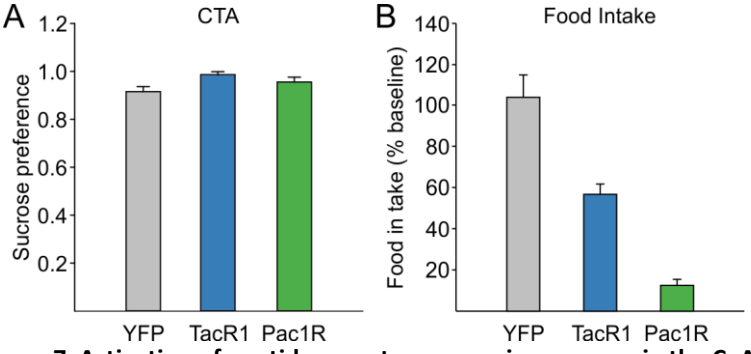

Figure 7. Activation of peptide receptor-expressing neurons in the CeA
(A) Pairing stimulation of TacR1 or Pac1R neurons with novel sucrose does not result in CTA.
(B) Activation of TacR1 and Pac1R neurons suppresses feeding.

As an alternative to Cre driver mouse lines, I also targeted CeA neurons activated by CGRP neurons as marked by Fos. This approach uses the $Fos^{2ACreERt}$ transgenic mouse, which has tamoxifen-inducible Cre recombinase fused to Fos but separated by a 2A peptide-cleavage sequence (Allen et al., 2017). Administration of 4-hydroxytamoxifen (4-OHT) will allow selective Cre expression in neurons that also express Fos during the time that 4-OHT is active. These mice were bred to $\underline{Calca^{Cre}}$ mice to create double-transgenic $Fos^{2ACreERt}::Calca^{Cre}$ mice. Next, AAV1-DIO-hM3Dq:mCherry was bilaterally injected into the PBN while AAV1-DIO-ChR2:YFP was injected into the CeA. Several weeks later, CGRP neurons were activated by an injection of CNO. At the same time, mice were also given an injection of 4-OHT so that neurons in the CeA that express Fos as a result of CGRP neuronal activation will also express Cre recombinase and turn on ChR2 expression. These mice were

conditioned using the CTA paradigm as described previously, with two pairings of sucrose and photostimulation of neurons in the CeA (Figure 8A). Using this approach, only 3/10 mice developed a robust CTA with sucrose preference below 0.2 (Figure 8B). Interestingly, the 3 mice that learned a CTA had very sparse viral labeling despite correct fiber-optic placement, indicating that the viral targeting was correct (Figure 8C) while the 4 mice that did not develop CTA (sucrose preference above 0.8) had robust ChR2 labeling in the CeA (Figure 8D). However, photoactivation of neurons in all mice, regardless of viral expression, was sufficient to decrease food intake (Figure 8C) and there was no correlation between level of CTA and change in food intake (Figure 8D).

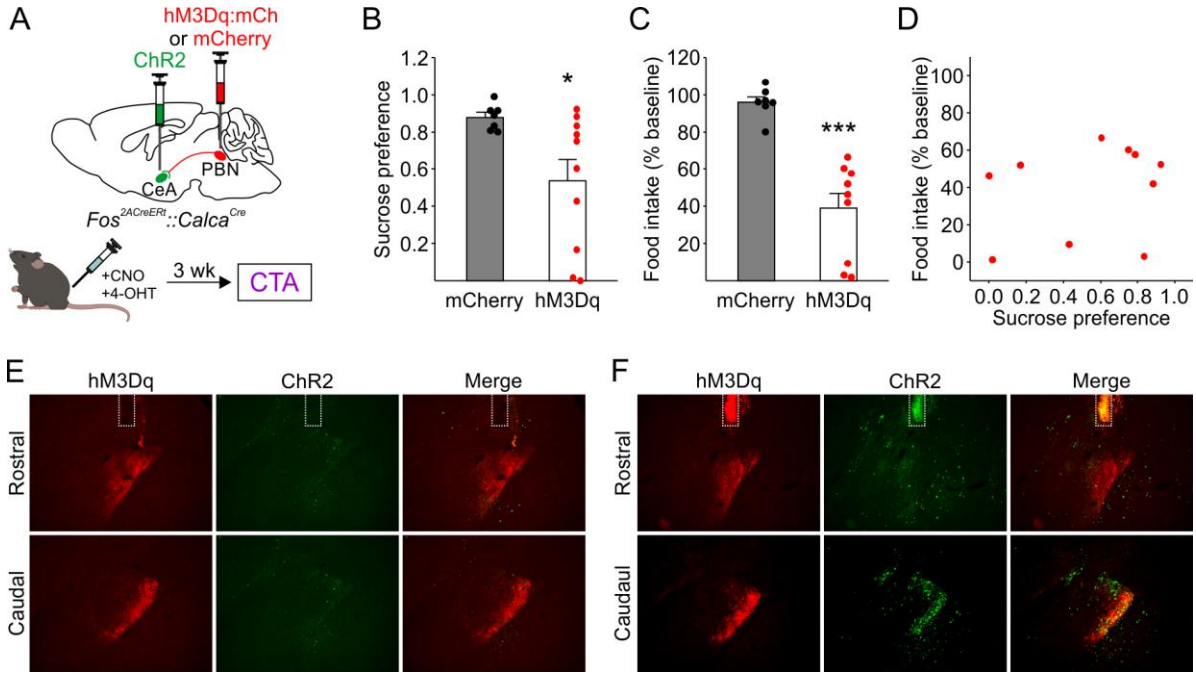

Figure 8. Targeting CeA neurons activated by CGRP stimulation.
(A) Diagram of viral injections and experiment design with *Fos*^{2ACreERt}*::Calca*^{Cre} mice.
(B) Pairing stimulation of CeA neurons activated by CGRP stimulation with novel sucrose results in a mild CTA (mCherry: n=7, hM3Dq: n=10, unpaired two-tailed Student's *t* test, *t*(15)=2.437, *P*=0.0277).
(C) Stimulation of CeA neurons decreased food intake (mCherry: n=7, hM3Dq: n=10, unpaired two-tailed Student's *t* test, *t*(15)=5.767, *P*<0.001).
(D) Correlation between food intake and sucrose preference after CTA (Pearson Correlation, r^2=0.55, *P*=0.478).
(E-F) Representative image of viral targeting in two mice showing hM3Dq:mCherry fibers from CGRP neurons in the PBN and ChR2:YFP expression in the CeA. White outline marks location of optic fiber placement.

Discussion

These data show that activation of Calcrl, TacR1, or Pac1R neurons in the CeA, as well as Fos-expressing neurons resulting from CGRP neuron stimulation was not sufficient to induce a CTA. This was surprising given that stimulation of CGRP terminals in the CeA is sufficient for CTA, indicating that a population of neurons downstream of CGRP neurons involved in CTA does exist, but remains to be identified. Activation of all of these neuronal populations produced an anorexic phenotype, which is biological evidence of effective neuron activation.

Our unpublished RiboTag data show enrichment of numerous neuropeptides within CGRP neurons, suggesting that activation of CGRP neurons not only induces release of glutamate, but also numerous neuropeptides that may influence behavior. CGRP itself is also important for the full expression of CTA, indicating that glutamate alone may not fully mediate this behavior. This idea guided our experiments towards activation of neurons that express receptors for each of these neuropeptides. However, it is possible that activation of these post-synaptic neurons by ChR2 or hM3Dq alone is not sufficient to recapitulate the effects of CGRP neuronal activation, which likely results in release of glutamate along with a variety of neuropeptides. Glutamate released from terminals diffuses rapidly across the synaptic cleft and quickly activate receptors on the postsynaptic membrane. Neuropeptides are released from both synaptic terminals and somato-dentritic varicosities and can act on multiple sites through diffusion in the extracellular space. Furthermore, neuropeptides also activate G-protein coupled receptors, which in turn activate a variety of signaling cascades that can have long-lasting effects on synaptic transmission (Alexander et al., 2009, Armbruster et al., 2007, Guettier et al., 2009). Thus, further understanding of the signaling pathways activated through CGRP neuronal activity are needed to more efficiently activate CeA neurons for CTA.

The observation that very sparse viral expression in the CeA from the $Fos^{2ACreERt}::Calca^{Cre}$ experiment was more effective in generating a CTA than dense expression suggests that activating

entire populations of neurons may actually interfere with CTA acquisition. In fact, neurons within the CeA have been shown to be heavily interconnected, with a dense population of both GABAergic interneurons and GABAergic projection neurons that inhibit each other (Pape and Pare, 2010). In addition to GABA and the neuropeptide receptors mentioned above, the CeA also contains neurons identified by a variety of genetic markers including somatostatin, protein kinase C-δ (PKC-δ), serotonin receptor 2a, corticotropin-releasing hormone, and tachykinin 2 (Cai et al., 2014, Li et al., 2013, Sanford et al., 2016, McCullough et al., 2018, Cornea-Hebert et al., 1999, Moga and Gray, 1985, Zirlinger et al., 2001). Furthermore, activation of neurons with the same genetic marker along the rostral-caudal extent of the CeA can produce differential behavior effects. For example, PKC-δ neurons, a subset of Calcrl neurons, in the rostral capsular CeA are activated by stimuli that result in defensive behaviors while PKC-δ in the caudal lateral CeA are activated during fear conditioning extinction (Kim et al., 2018). Not only do these two populations of PKC-δ neurons have opposing effects on defensive behavior, they are also reciprocally connected (Kim et al., 2018). Thus, bulk activation of a large number of neurons in the CeA may have opposing effects on CTA, thereby interfering with the transmission of US signals from CGRP neurons in the PBN.

Conclusions

The goal of this thesis is to delineate the role of CGRP neurons and their downstream projections in the acquisition and expression of CTA, and to identify the genetic identity of neurons in the CeA that mediate CTA. Previous work in the lab had demonstrated that photoactivation of CGRP neurons in the PBN was sufficient to substitute for the US signal in CTA and that inactivation of these neurons greatly attenuated CTA. The experiments described here extended these studies by demonstrating that:

1. A robust and long-lasting CTA can be induced with both LiCl and LPS injections as the US.
2. Chemogenetic activation of CGRP neurons also results in CTA.
3. The strength of CTA induced by CGRP neuron activation depends on stimulation frequency and duration.
4. Two major forebrain targets of CGRP neurons (CeA and BNST) can generate a robust CTA.
5. CTA results in synaptic plasticity of CGRP neurons and requires Arc and NMDA signaling.
6. CGRP neurons are re-activated by the conditioned taste after CTA learning.
7. Transient inactivation or permanent silencing of CGRP neurons prevents expression of CTA.
8. Activation of Calcrl neurons in the CeA suppresses feeding and induces place aversion in a frequency-dependent manner but does not result in CTA.
9. CTA does not occur after activation of Calcrl, TacR1, Pac1R neurons in the CeA.

Future Directions

These experiments show that CGRP neurons in the PBN are essential for both the acquisition and expression of a CTA, confirming that they are a critical component of the CTA neural circuitry. However, it is still unclear which region downstream of CGRP neurons is necessary for transmitting the US signal underlying acquisition of a CTA. The experiments on neurons in the CeA indicate that while stimulation many neurons can result in suppression of feeding, this does not necessarily result in learning a CTA. Because none of the candidate genes that we tested resulted in CTA and the experiments using $Fos^{2ACreERt}$ mice yielded conflicting results, it is important to use an unbiased method of targeting CeA neurons that are directly downstream of CGRP neurons. Existing techniques for cell-type specific trans-synaptic targeting of neurons rely largely on a pseudo-rabies virus, which results in high cytotoxicity within a week and precludes its use in long-term behavioral experiments (Wickersham et al., 2007, Kim et al., 2016). Though recent modifications have resulted in second-generation rabies viruses that appear to have no toxic effects (Chatterjee et al., 2018), their efficacy for behavioral experiments has not been validated.

An alternative approach to targeting post-synaptic neurons is to utilize wheat germ agglutinin (WGA), which can transport fluorophores in both an anterograde and retrograde manner (Yoshihara 2002, Broadwell and Balin, 1985, Fabian and Coulter, 1985). Our lab has created a construct that will allow WGA transport of Cre recombinase in a Cre-dependent manner. Briefly, a loxP-flanked stop cassette was inserted into the open reading frame of Cre recombinase that is fused to WGA (Figure 9A).

Action of Cre will remove the stop sequence and allow expression of Cre, which will be transported by WGA to upstream and downstream targets (Figure 9B). This construct, when injected into the PBN of *Calca*^{Cre} mice, has been demonstrated to allow Cre-dependent expression of AAV1-DIO-YFP in the CeA (Figure 9C and 9D), and is a promising tool in capturing neurons downstream of CGRP that mediate CTA. Once CTA has been established in CeA neurons, this virus can be used to express RiboTag to identify the genetic markers that mediate CTA in the CeA. Alternatively, single-cell RNA sequencing methods can also be used.

However, perhaps the biggest pitfall of this approach stems from the interconnectivity of the CeA and PBN (Jia et al., 2005, Cai et al., 2014, Moga and Gray, 1985). Although WGA is traditionally used as an anterograde tracer, it has also been reported to move in a retrograde direction (Yoshihara, 2002). Therefore, it is possible that CeA neurons that are upstream of CGRP, rather than downstream, are labeled by this approach (Figure 10). Subsequent stimulation of this population of CeA neurons would ultimately result in re-activation of CGRP neurons in

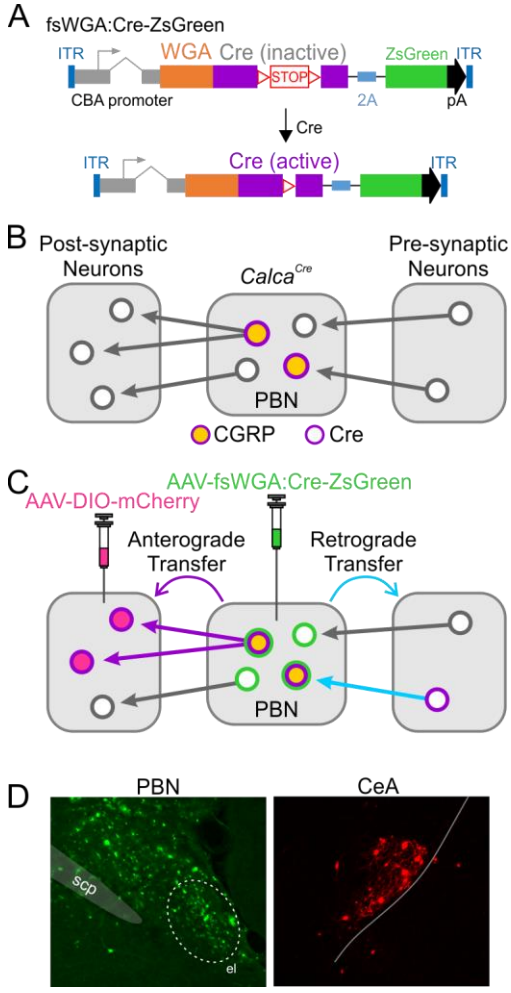

Figure 9. Illustration of WGA approach. (A) Cre-dependent WGA construct, fsWGA:Cre-ZaGreen (B) *Calca*^{Cre} neurons in the PBN receive both pre- and post-synaptic input (C) Injection of fsWGA:Cre-ZsGreen into the PBN and DIO-mCherry into the CeA (D) Expression of ZsGreen in the PBN and mCherry positive cells in the CeA.

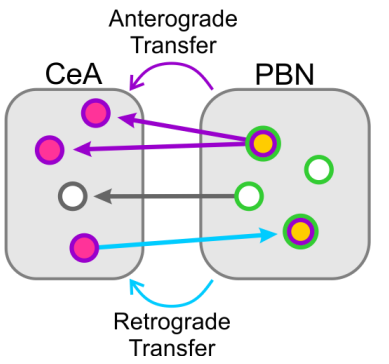

Figure 10. Caveat of WGA approach in the CeA.

the PBN, rather than extending the circuitry to downstream regions. Thus, the efficacy of this virus in labeling post-synaptic neurons will need to be verified with slice electrophysiology or other tracing methods.

Our observation that none of the neuronal populations tested in the CeA resulted in CTA may suggest that other downstream targets are involved. Since stimulation of $CGRP^{PBN}$ projections to either the CeA or BNST can result in CTA, there may be redundant circuitry involved in CTA learning. In agreement, previous studies have shown that lesions of the CeA or BNST have no effect on learning a CTA (Morris et al., 1999, Reilly and Bornovalova, 2005, Roman et al., 2006, Yamamoto et al., 1995). This may be due to the reciprocal connections within the CeA and BNST (Douglass et al., 2017, Gungor et al., 2015, Yu et al., 2017), as well as their nearly identical inputs and target projections (Haufler et al., 2013, Lebow and Chen, 2016, Ye and Veinante, 2019). Alternatively, it is possible that activation of CGRP projections in the CeA is also activating fibers of passage that terminate in the BNST. One experiment that can address this issue is to inactivate CeA neurons, either the entire population or in specific neurons such as Calcrl, $Fos^{2ACreERt}::Calca^{Cre}$ mice, or with the fsWGA virus, while stimulating CGRP projections in the CeA. If this manipulation still results in a CTA, it would suggest that the CeA is not critical for CTA learning. Although many studies have focused on the amygdala as a point of convergence between the taste and visceral malaise signals (Reilly and Bornovalova, 2005), our data suggest that this CS-US association may form in multiple sites to give rise to a CTA.

Finally, in vivo calcium imaging experiments have shown that CGRP neurons respond to wide variety of threats in addition to visceral malaise including noxious heat and painful stimuli. Activation of CGRP neurons can also substitute for the foot shock as a US during fear conditioning while inactivation attenuates responses to aversive stimuli (Campos et al., 2018). These findings suggest that CGRP neurons not only relay malaise, but act as a general alarm for potential threats to the animal. As CTA and fear conditioning are discrete behaviors that lead to activation of different circuits (e.g., taste vs

auditory pathways), future experiments can aim to elucidate how circuits downstream of CGRP neurons diverge to form distinct taste aversion and fear memories. Learning the association between food and illness requires the coordinated activity of not only the taste and malaise neural circuitry, but also other pathways involved in stress, reward, and homeostasis. Thus, understanding the neural integration of taste and malaise can provide insight into how different systems in the brain interact to promote our well-being.

Methods

Experimental Model and Subject Details. All experiments were approved by the University of Washington Institutional Animal Care and Use Committee and were performed in accordance with the guidelines described in the US National Institutes of Health Guide for the Care and Use of Laboratory Animals. All mice were backcrossed for > 6 generations onto a C57Bl/6 background. *Calca*$^{Cre/Cre}$, *Calca*$^{Cre/+}$, and *Grin1*$^{lox/lox}$ mice were generated as described previously (Carter et al., 2013, Tsien et al., 1996). *Calca*$^{frtCre/frtCre}$*::Grin1*$^{lox/lox}$ males were bred with *Grin1*$^{lox/+}$ females and *Calca*$^{frtCre/frtCre}$*::Arc*$^{lox/lox}$ males were bred with *Arc*$^{lox/+}$ females to generate KO and heterozygous (HET) control mice . Knockout and control mice were identified by PCR of tail DNA. Both male and female mice were used for all experiments, aged 7-9 weeks at the start of experimental procedures and no more than 20 weeks at the end of experimental procedures. Mice were housed on a 12-h light/dark cycle (lights on 05:00-17:00) at ~22°C with food and water available *ad libitum*, except during CTA and food- intake studies described below. Animals from the same litter were split randomly between control and experimental groups, with an equal number of male and female mice in each group.

Design of *Calca*-FLP-dependent Cre Recombinase. A FLP-dependent Cre recombinase was constructed by inserting a *Mt1* gene intron within the open reading frame of mnCre:GFP, which has a Myc tag (m), followed by a nuclear localization signal (NLS, n), followed by Cre recombinase fused to green fluorescent protein (Cre:GFP), to generate a gene with two exons. Then the second exon was inverted and flanked by a pair of dissimilar frt sites to make a DIO construct. The action of FLP recombinase inverts the second exon allowing splicing to generate functional Cre recombinase. This cassette was substituted for Cre:GFP in the *Calca*$^{Cre:GFP}$ construct described previously (Carter et al., 2013) to generate

Calca^{frtCre} mice (Figures S3B-D). Mice with this construct were generated as described (Carter et al., 2013).

Generation of Conditional *Arc* Mice. To make the targeting construct, the 5' arm (~7.5 kb with *Pac*1 and *Sal*1 sites at each end) and the 3' arm (~5 kb with *Pme*1 and *Not*1 sites) were PCR amplified with Q5 DNA polymerase from a mouse C57Bl/6 BAC clone. These arms were cloned into the polylinkers of targeting vector that includes a loxP site, frt-flanked Sv-Neo gene for positive selection and *Pgk*-DTa and HSV-TK genes for negative selection. A loxP site was inserted into the *BssH*1 site in the *Arc* promoter region; the other loxP site is in the first intron downstream of the first exon, which includes entire coding region (Figure S3A). Thus, Cre-mediated recombination removes the entire coding region. This construct was electroporated into G4 ES cells (C57Bl/6 x 129/Sv hybrid); DNA from clones was digested with *Nsi*1 subjected to Southern blot procedure using a radioactive probe located outside of the 5' arm. Eight of 82 clones analyzed were correctly targeted, but only one retained the 5' loxP site. That clone was injected into blastocysts that were then transplanted into foster mothers. Chimeric pups that were positive for the transgene were bred with Rosa26-FLPer to remove the SV-Neo gene and then with C57Bl/6 mice to remove Rosa26-FLPer. Genotyping was performed using a pair of primers that flank the 5' loxP site.

Virus Production. pAAV-hSyn-DIO-hM3Dq:mCherry, pAAV-Ef1α-DIO-mCherry, and pAAV-hSyn-dF-HA-KORD:mCitrine DNA plasmids were provided by B. Roth (Addgene, plasmids #44361, #50462, #65417). pAAV-Ef1α-DIO-ChR2:YFP and pAAV-hSyn-DIO-YFP DNA plasmids were provided by K. Deisseroth (Stanford University). pAAV-Ef1α-DIO-synaptophysin:mCherry DNA plasmid was generated from pAAV-Ef1α-DIO-synaptophysin:GFP by replacing the GFP fragment with mCherry (Roman et al., 2016). pAAV-CBA-Flippase:DsRed and pAAV-CBA-DIO-GCamp6m DNA plasmids were provided by L. Zweifel. Viruses

were prepared in-house by transfecting HEK cells with an AAV1 coat stereotype, purified by sucrose and CsCl gradient centrifugation steps, and re-suspended in 0.1 M phosphate-buffered saline (PBS).

Stereotaxic Surgery. Mice were anesthetized with isoflurane and placed on a robotic stereotaxic frame (Neurostar). Virus was injected unilaterally or bilaterally as described in the text in the PBN (antero-posterior (AP) -5.00 mm; medio-lateral (ML) +/-1.35 mm; dorso-ventral (DV) 3.40) at a rate of 0.2 µl/min for 2.5 min. In mice used for optogenetic experiments, two custom-made fiber optic cannulas were implanted bilaterally above the PBN (AP -5.00 mm, ML +/- 1.75 mm, DV 3.0), CeA (AP, -1.20 mm, ML +/- 2.9 mm, DV 4.50 mm), BNST (AP 0.14 mm, ML +/- 1.20 mm, DV 4.00 mm), or VPMpc (AP -1.80 mm, ML +/- 1.25 mm, DV 3.00 mm) and affixed to the skull with C&B Metabond (Parkell) and dental acrylic. Mice were allowed to recover for 3 to 5 wk before start of behavioral tests.

Photostimulation. After recovery from surgery, mice were acclimated to dummy cables attached to the implanted fiber optic cannulas. For CTA and food-intake studies, bilateral branching fiber optic cables (200-µm diameter, Doric Lenses) were attached to the head of each mouse before presentation of sucrose or food. Light-pulse trains (10 ms; 3 s on, 2 s off) were delivered at 5 Hz or 30 Hz for 5, 30, or 120 min as described in the text. Stimulation paradigms were programmed using a Master8 (AMPI) pulse stimulator that controlled a blue-light laser (473 nm; LaserGlow). The power of light exiting each side of the branching fiber optic cable was adjusted to 10 ± 1 mW.

Conditioned taste Aversion (CTA) Assay. Mice were individually housed in custom cages with angled ports for placement of 2 test tubes of water. After 7 d of acclimation to the cage and bottles, mice were water deprived overnight. On days 1-3, mice had access to water for 30 min approximately 4 h after the onset of the light cycle and for 1 h before the onset of the dark cycle. On day 4, mice were given 30 min

access to a novel 5% sucrose solution, followed by an injection of LiCl, LPS, CNO, or photostimulation. Water was available for 1 h in the afternoon and again on day 5, following the same schedule as days 1-3. This conditioning was repeated on days 6 and 7. On day 8, mice were given access to two bottles (water and 5% sucrose) for 30 min. The volume consumed was recorded in grams and converted to milliliters.

For calcium imaging and TetTox experiments, *ad libitum*-fed mice were presented with a test tube of vanilla-flavored Ensure approximately 2 h after the onset of the light cycle. Twenty min after the first lick, mice were injected with LPS and the Ensure bottle was removed after 4 h. Activity of $CGRP^{PBN}$ neurons was measured on the second re-exposure to Ensure. Surgery on mice for TetTox experiments was performed 3 or 4 d after conditioning and mice were allowed to recover for 3 wk before testing for CTA.

Measuring Food Intake. After CTA, mice were allowed to recover for 7 d with *ad libitum* access to food and water. During this time, mice were also acclimated to a different rodent diet (D12450B, Research Diets), which was less susceptible to crumbling during consumption.

For manipulations of $CGRP^{PBN}$ neurons with CNO and SalB, mice were acclimated to BIODAQ recording chambers (Research Diets) for 7 d. Food was removed 5 h prior to the start of the dark cycle each day and returned 15 min after lights out. Baseline food intake was measured for 3 d after the acclimation period and averaged. The next day, mice were given an injection of CNO 15 min prior to the start of the dark cycle and an injection of SalB at lights out. Food was returned 15 min into the dark cycle and consumption was measured overnight.

For photostimulation of $CGRP^{PBN}$ fibers, mice were fasted overnight then food restricted to 90% of their pre-fasting body weight for 3-4 d. During baseline food-intake measurements, optic fibers were bilaterally connected to the fiber-optic cannulas on the head of mice but no laser stimulation was given.

Mice were given access to food for 2 h and the amount consumed was recorded. The next day, mice were photostimulated for 30 min at 30 Hz and food consumed over 2 h was recorded.

Calcium imaging. Mice were prepared for calcium imaging as described (Resendez et al., 2016). Briefly, 3 wk after viral injection, mice were anesthetized with isoflurane and implanted with a microendoscope lens (6.1 mm length, 0.5 mm diameter; Inscopix #100-000588) with assistance of a ProView implant kit (Inscopix, #100-000754) that allowed visualization of fluorescent activity during implantation. The lens was targeted to be ~200–300 µm above the neurons using the following coordinates: AP -4.80 mm, ML -1.70 mm, DV 3.20 mm. One week after lens implantation, mice were anesthetized and a baseplate (Inscopix, #100-000279) was implanted above the lens. The baseplate provides an interface for attaching the miniature microscope during calcium imaging experiments, but at other times a baseplate cover (Inscopix, #100-000241) was attached to prevent damage to the microendoscope lens. Calcium fluorescence was recorded at 5 frames/s. The recording parameters were based on pilot studies that demonstrated the least amount of photobleaching while allowing sufficient detection of fluorescent activity. Ethovision XT10 (Noldus Technology) was used to trigger and synchronize calcium recordings with behavioral video recordings.

Slice Electrophysiology. Mice were deeply anesthetized with isoflurane and intracardially perfused with 10 ml of cold (4-6 °C) cutting solution containing (in mM): 92 NMDG, 2.5 KCl, 1.25 NaH_2PO_4, 30 $NaHCO_3$, 20 HEPES, 25 D-glucose, 2 thiourea, 5 Na-ascorbate, 3 Na-pyruvate, 0.5 $CaCl_2$, 10 $MgSO_4$. Coronal slices (200 µm) were prepared using a vibrating microtome (VT1000S, Leica Biosystems) then allowed to recover for 10 min at 32 °C in the same cutting solution. Slices were then transferred to a room temperature recovery solution containing (in mM): 92 NaCl, 2.5 KCl, 1.25 NaH_2PO_4, 30 $NaHCO_3$, 20 HEPES, 25 D-glucose, 2 thiourea, 5 Na-ascorbate, 3 Na-pyruvate, 2 $CaCl_2$, 2 $MgSO_4$ and allowed to

recover for an additional 45 minutes. Recordings were made in artificial cerebral spinal fluid containing (in mM): 126 NaCl, 2.5 KCl, 1.2 NaH_2PO_4, 18 $NaHCO_3$, 11 D-glucose, 2.4 $CaCl_2$, 1.2 $MgCl_2$ continuously perfused at a rate of ~2 ml/min at 32 °C. All solutions were continuously oxygenated with 95% O_2-5% CO_2 (pH 7.3-7.4, 300-310 mOsm). Whole cell patch-clamp recordings were obtained using a MultiClamp 700B amplifier (Molecular Devices) and filtered at 1 kHz. Only data from cells with series resistance values <25 MΩ which did not vary > 20% during the experiment were included in data analysis.

For spontaneous EPSCs and AMPA/NMDA currents, bicuculline (10 µM) was included in the bath and patch electrodes (3-5 MΩ) were filled with an internal solution containing and (in mM): 120 $CsMeSO_3$, 20 HEPES, 0.4 EGTA, 2.8 NaCl, 2.5 Mg-ATP, 0.25 Na-GTP, 5 QX-314 bromide, pH 7.3, 290 mOsm. Electrodes also contained 0.2% biocytin to label recorded cells. CGRP neurons, as identified by GFP or mCherry epifluorescence, were held at V_{hold}= -70 mV and spontaneous EPSCs were recorded for 1 min. A concentric bipolar electrode placed in the superior cerebellar peduncle delivered 1 ms stimuli at 0.1 Hz to elicit AMAPR-mediated currents. 15 traces were average per cell then V_{hold} was stepped to +40 mV. NMDAR-mediated currents were measured as the average EPSC amplitude between 11 and 15 ms following the stimulus artifact, after the AMPA component had largely decayed. After the experiment, slices were fixed in 4% paraformaldehyde (PFA) overnight then cryoprotected in 30% sucrose and frozen for histology.

For recording of action potentials following current injection, patch pipettes were filled with an internal solution containing (in mM): 130 K-gluconate, 10 HEPES, 5 NaCl, 1 EGTA, 5 Mg-ATP, 0.5 Na-GTP, pH 7.3, 290 mOsm.

Evoked AMPA/NMDA currents and action potentials were analyzed offline using Clampfit 10.3 (Axon Instruments) software. Spontaneous EPSCs were analyzed with an automated detection protocol in MiniAnalysis (Synaptosoft) and manually checked for accuracy.

Pharmacological injections. All pharmacological agents, with the exception of SalB, were prepared in sterile water and administered intraperitoneally (i.p.). These include: LiCl (0.2 M at 15 ml/kg; Fisher #L121), LPS, *S. typhimurium* (50 µg/kg; Calbiochem, #437650), and CNO (1 mg/kg; RTI #C929). SalB (10 mg/kg; Cayman Chemical #11488) was dissolved in DMSO and injected subcutaneously as described (Vardy et al., 2015).

Histology and Microscopy. Mice were anesthetized with Beuthansia (0.2 ml, i.p.; Merck) and perfused transcardially with PBS followed by 4% PFA in PBS. Brains were post-fixed overnight in 4% PFA at 4°C, cryoprotected in 30% sucrose, frozen in OCT compound (ThermoFisher), and stored at -80°C. Coronal sections (30 µm) were cut on a cryostat (Leica Microsystems) and collected in cold PBS. For Fos studies, mice were photostimulated for 15 min or given CNO and/or SalB 90 min before perfusion.

For immunohistochemistry experiments, sections were washed three times in PBS with 0.2% Triton X-100 (PBST) for 5 min and incubated in blocking solution (3% normal donkey serum in PBST) for 1 h at room temperature. Sections were incubated overnight at 4°C in PBST with primary antibodies including: rabbit anti-c-Fos (1:2000, Abcam, ab190289), goat anti-c-Fos (1:500, Santa Cruz Biotechnology, sc-52), chicken-anti-GFP (1:10000, Abcam, ab13970), and/or mouse-anti-CGRP (1:1000, Abcam, ab 81887). Slices from electrophysiology experiments were incubated in streptavidin conjugated to marina blue (1:2000, ThermoFisher, S11221). After 3 washes in PBS, sections were incubated for 1 h in PBS with secondary antibodies: Alexa Fluor 488 donkey anti-chicken, Alexa Fluor 594 donkey anti-mouse, Cy5 donkey anti-goat, and/or Cy5 donkey anti-rabbit (1:500, Jackson ImmunoResearch). Tissue was washed 3 times in PBS, mounted onto glass slides, and coverslipped with Fluoromount-G (Southern Biotech).

Fluorescent images were acquired using a Keyence BZ-X700 microscope. Images were minimally processed using ImageJ software (NIH) to enhance brightness and contrast for optimal representation of

the data. All digital images were processed in the same way between experimental conditions to avoid artificial manipulation between different data sets.

Quantification and Statistical Analysis.

An online power and sample size calculator was used to determine an effective sample size for statistical comparisons (http://powerandsamplesize.com). Based on a pilot study for CTA, we used a mean sucrose preference of 0.4 and s.d. of 0.2. Assuming a significance level of 0.05 and power of 0.8, we calculated a sample size of 4 mice per group if means were 2-fold different with a two-tailed Student's t test. SigmaPlot 12.0 (Systat Software) was used for all other statistical analysis. For all data, normality was tested using the Shapiro-Wilk test to determine whether parametric or non-parametric analyses were required. The asterisks in the figures represent the P-values of post hoc tests corresponding to the following values *P<0.05, **P<0.01, ***P<0.001. Data and figures were exported into CorelDraw X6 (Corel) for preparation of figures.

Following imaging, any mouse whose targeted injection site was missed or demonstrated very sparse expression (≤10 fluorescent neurons/section at Bregma -5.1) was excluded from experimental analysis.

References

Allen, W.E., DeNardo, L.A., Chen, M.Z., Liu, C.D., Loh, K.M., Fenno, L.E., Ramakrishnan, C., Deisseroth, K., & Luo, L. (2017) Thirst-associated preoptic neurons encode an aversive motivational drive. *Science* 357, 1149-55.

Alexander, G.M., Rogan, S.C., Abbas, A.I., Armbruster, B.N., Pei, Y., Allen, J.A., Nonneman, R.J., Hartmann, J., Moy, S.S., Nicoleis, M.A., McNamara, J.O., & Roth, B.L. (2009). Remote control of neuronal activity in transgenic mice expressing evolved G protein-coupled receptors. *Neuron* 63, 27-39.

Armbruster, B.N., Li, X., Pausch, M.H., Herlitze, S., & Roth, B.L. (2007). Evolving the lock to fit the key to create a family of G protein-coupled receptors potently activated by an inert ligand. *Proc Natl Acad Sci U S A* 104, 5163-8.

Bernstein, I.L. (1985). Learned food aversions in the progression of cancer and its treatment. *Annals of the New York Academy of Sciences* 443, 365-380.

Boakes, R.A., Tarrier, N., Barnes, B.W., & Tattersall, M.H. (1993). Prevalence of anticipatory nausea and other side-effects in cancer patients receiving chemotherapy. *European journal of cancer* 29A, 866-870.

Bonacchi, K.B., Ackroff, K., & Sclafani, A. (2008). Sucrose taste but not Polycose taste conditions flavor preferences in rats. *Physiology & behavior* 95, 235-244.

Broadwell, R.D., & Balin, B.J. (1985) Endocytic and exocytic pathways of the neuronal secretory process and trans-synaptic transfer of wheat germ agglutinin-horseradish peroxidase in vivo. *J Comp Neurol* 242, 632-50.

Brett, L.P., Hankins, W.G., & Garcia, J. (1976). Prey-lithium aversions. III: Bueto hawks. *Behavioral biology* 17, 87-98.

Cai, H., Haubensak, W., Anthony, T.E., & Anderson, D.J. (2014) Central amygdala PKC-δ(+) neurons mediate the influence of multiple anorexigenic signals. *Nat Neurosci* 17, 1240-8.

Campos, C. A., Bowen, A. J., Roman, C. W. & Palmiter, R. D. (2018). Encoding of danger by parabrachial CGRP neurons. *Nature* 555**,** 617-622.

Campos, C. A., Bowen, A. J., Schwartz, M. W. & Palmiter, R. D. (2016). Parabrachial CGRP Neurons Control Meal Termination. *Cell Metab* 23**,** 811-20.

Cannon, D.S., Best, M.R., Batson, J.D., & Feldman, M. (1983). Taste familiarity and apomorphine-induced taste aversions in humans. *Behaviour research and therapy* 21, 669-673.

Carter, M. E., Han, S. & Palmiter, R. D. (2015). Parabrachial calcitonin gene-related peptide neurons mediate conditioned taste aversion. *J Neurosci* 35**,** 4582-6.

Carter, M. E., Soden, M. E., Zweifel, L. S. & Palmiter, R. D. (2013). Genetic identification of a neural circuit that suppresses appetite. *Nature* 503**,** 111-4.

Chatterjee, S., Sullivan, H.A., MacLennan, B.J., Xu, R., Hou, Y., Lavin, T.K., Lea, N.E., Michalski, J.E., Babcock, K.R., Dietrich, S., Matthews, G.A., Beyeler, A., Calhoon, G.G., Glober, G., Whitesell, J.D., Yao, S., Cetin, A., Harris, J.A., Zeng, H., Tye, K.M., Reid, R.C., & Wickersham, I.R. (2018) Nontoxic, double-deletion-mutant rabies viral vectors for retrograde targeting of projection neurons. *Nat Neurosci* 21, 638-46.

Chen, T., Zhu, J., Yang, L. K., Feng, Y., Lin, W. & Wang, Y. H. (2017). Glutamate-induced rapid induction of Arc/Arg3.1 requires NMDA receptor-mediated phosphorylation of ERK and CREB. *Neurosci Lett* 661**,** 23-28.

Cornea-Hebert, V., Riad, M., Wu, C., Singh, S.K., & Descarries, L. (1999) Cellular and subcellular distribution of the serotonin 5-HT2A receptor in the central nervous system of adult rat. *J Comp Neurol* 409, 187-209.

Critchley, H.D., & Harrison, N.A. (2013). Visceral influences on brain and behavior. *Neuron 77*, 624-638.
Douglass, A. M., Kucukdereli, H., Ponserre, M., Markovic, M., Grundemann, J., Strobel, C., Alcala Morales, P. L., Conzelmann, K. K., Luthi, A. & Klein, R. (2017). Central amygdala circuits modulate food consumption through a positive-valence mechanism. *Nat Neurosci* 20**,** 1384-1394.
Dragoin, W.B., McCleary, G.E., & McCleary, P. (1971). A comparison of two methods of measuring conditioned taste aversions. *Behav Res Meth Instrum 3*, 309-310.
Dwyer, D. M., Gasalla, P., Bura, S. & Lopez, M. (2017). Flavors paired with internal pain or with nausea elicit divergent types of hedonic responses. *Behav Neurosci* 131**,** 235-48.
Elkins, R.L. (1973). Individual differences in bait shyness: effects of drug dose and measurement technique. *Physiol Record* 23, 349-358.
Fabian, R.H., & Coulter, J.D. (1985) Transneuronal transport of lectins. *Brain Res* 344, 41-8.
Fanselow, M. S. & Wassum, K. M. (2015). The Origins and Organization of Vertebrate Pavlovian Conditioning. *Cold Spring Harb Perspect Biol* 8**,** a021717.
Flynn, F.W., Grill, H.J., Shulkin, J., & Norgren, R. (1991). Central gustatory lesions. II. Effects on sodium appetite, taste aversion learning, and feeding behavior. *Behavioral Neuroscience* 105, 933-943.
Fox, R.A., Corcoran, M., & Brizzee, K.R. (1990). Conditioned taste aversion and motion sickness in cats and squirrel monkeys. *Canadian journal of physiology and pharmacology* 68, 269-278.
Gal-Ben-Ari, S., & Rosenblum, K. (2011). Molecular mechanisms underlying memory consolidation of taste information in the cortex. *Frontiers in behavioral neuroscience* 5, 87.
Garb, J.L., & Stunkard, A.J. (1974). Taste aversions in man. *The American journal of psychiatry* 131, 1204-1207.
Garcia, J., Kimeldorf, D. J. & Koelling, R. A. (1955). Conditioned aversion to saccharin resulting from exposure to gamma radiation. *Science* 122**,** 157-8.
Garcia, J. & Koelling, R. A. (1966). Relation of cue to consequence in avoidance learning. *Psychonomic Sci* 4**,** 123-4.
Garcia, J., & Koelling, R.A. (1967). A comparison of aversions induced by x-rays, toxins, and drugs in the rat. *Radiation research Supplement* 7, 439-450.
Gauriau, C., & Bernard, J.F. (2001) Pain pathways and parabrachial circuits in the rat. *Experimental Physiol* 87.2, 251-258.
Grill, H. J. & Norgren, R. (1978). Chronically decerebrate rats demonstrate satiation but not bait shyness. *Science* 201**,** 267-9.
Grigson, P.S. (1997). Conditioned taste aversions and drugs of abuse: a reinterpretation. *Behavioral neuroscience* 111, 129-136.
Guettier, J.M., Gautam, D., Scarselli, M., Ruiz de Azua, I., Li, J.H., Rosemond, E., Ma, X., Gonzalez, F.J., Armbruster, B.N., Lu, H., Roth, B.L., & Wess, J. (2009). A chemical-genetic approach to study G protein regulation of beta cell function in vivo. *Proc Natl Acad Sci U S A* 106, 19197-202.
Gungor, N. Z., Yamamoto, R. & Pare, D. (2015). Optogenetic study of the projections from the bed nucleus of the stria terminalis to the central amygdala. *J Neurophysiol* 114**,** 2903-11.
Gustavson, C.R., Jowsey, J.R., & Milligan, D.N. (1982). A 3-year evaluation of the taste aversion coyote control in Saskatchewan. *J Range Mgmt* 35, 57-59.
Hamamura, T., Lee, Y., Ohashi, K., Fujiwara, Y., Miki, M., Suzuki, H., & Kuroda, S. (2000) A low dose of lithium chloride selectively induces fos protein in the central nucleus of the amygdala of rat brain. *Prog Neuropsychopharmacol Biol Pychiatry* 24, 285-94.
Han, S., Soleiman, M. T., Soden, M. E., Zweifel, L. S. & Palmiter, R. D. (2015). Elucidating an Affective Pain Circuit that Creates a Threat Memory. *Cell* 162**,** 363-374.
Haufler, D., Nagy, F. Z. & Pare, D. (2013). Neuronal correlates of fear conditioning in the bed nucleus of the stria terminalis. *Learn Mem* 20**,** 633-41.

Houpt, K.A., Zahorik, D.M., & Swartzman-Andert, J.A. (1990). Taste aversion learning in horses. *Journal of animal science* 68, 2340-2344.
Ingram, D. K. (1982). Lithium chloride-induced taste aversion in C57BL/6J and DBA/2J mice. *J Gen Psychol* 106**,** 233-49.
Jia, H.G., Zhang, G.Y., & Wan., Q. (2005) A GABAergic projection from the central nucleus of the amygdala to the parabrachial nucleus: an unltrastructural stud of anterograde tracing in combination with post-embedding immunocytochemistry in the rat. *Neurosci Lett* 328, 153-7.
Jimenez, B., & Tapia, R. (2004). Biochemical modulation of NMDA receptors: role in conditioned taste aversion. *Neurochemical research* 29, 161-168.
Johansen, J. P., Cain, C. K., Ostroff, L. E. & Ledoux, J. E. (2011). Molecular mechanisms of fear learning and memory. *Cell* 147**,** 509-24.
Kim, E.J., Jacobs, M.W., Ito-Cole, T., & Callaway, E.M. (2016) Improved monosynaptic neural circuit tracing using engineered rabies virus glycoproteins. *Cell Reports* 15, 692-9.
Kim, J., Zhang, X., Muralidhar, S., LeBlanc, S.A., & Tonegawa, S. (2017) Basolateral to central amygdala neural circuits for appetitive behaviors. *Neuron* 93, 1464-79.
Koh, M.T., Wilkins, E.E., & Bernstein, I.L. (2003). Novel tastes elevate c-fos expression in the central amygdala and insular cortex: implication for taste aversion learning. *Behavioral neuroscience* 117, 1416-1422.
Krahn, D. D., Gosnell, B. A., Levine, A. S. & Morley, J. E. (1986). The effect of calcitonin gene-related peptide on food intake involves aversive mechanisms. *Pharmacol Biochem Behav* 24**,** 5-7.
Krashes, M.J., Koda, S., Ye, C., Rogan, S.C., Adams, A.C., Cusher, D.S., Maratos-Flier, E., Roth, B.L. & Lowell, B.B. (2011). Rapid, reversible activation of AgRP neurons drives feeding behavior in mice. *J Clin Invest* 121, 1424-8.
Lebow, M. A. & Chen, A. (2016). Overshadowed by the amygdala: the bed nucleus of the stria terminalis emerges as key to psychiatric disorders. *Mol Psychiatry* 21**,** 450-63.
Li, H., Penzo, M.A., Taniguchi, H., Kopec, C.D., Huang. Z.J., & Li, B. (2013) Experience-dependent modification of a central amygdala fear circuit. *Nat Neurosci* 16, 332-9.
Logue, A.W., Ophir, I., & Strauss, K.E. (1981). The acquisition of taste aversions in humans. *Behaviour research and therapy* 19, 319-333.
Lundy, R. F. & Norgren, R. (2015). *Gustatory System,* Waltham, MA, Academic Press, 891-921.
Martin, G.M., and Lett, B.T. (1985). Formation of associations of colored and flavored food with induced sickness in five avian species. *Behavioral and neural biology* 43, 223-237.
Mattis, J., Tye, K.M., Ferenczi, E.A., Ramakrishnan, C., O'Shea, D.J., Prakash, R., Gunaydin, L.A., Hyun, M., Fenno, L.E., Gradinaru, V., Yizhar, O. & Deisseroth, K. (2011). Principles for applying optogenetic tools derived from direct comparative analysis of microbial opsins. *Nat Methods* 9, 159-72.
Maren, S. (2005). Synaptic mechanisms of associative memory in the amygdala. *Neuron* 47**,** 783-6.
McCullough, K.M., Morrison, F.G., Hartmann, J., Carlezon, W.A., & Ressler, K.J. (2018) Quantified coexpression analysis of central amygdala subpopulations. *eNeuro* 0010-18.2018.
Moga, M.M. & Gray, T.S. (1985) Evidence for corticotropin-releasing factor, neurotensin, and somatostatin in the neural pathway from the central nucleus of the amydala to the parabrachial nucleus. *J Comp Neurol* 241, 275-84.
Morris, R., Frey, S., Kasambira, T. & Petrides, M. (1999). Ibotenic acid lesions of the basolateral, but not the central, amygdala interfere with conditioned taste aversion: evidence from a combined behavioral and anatomical tract-tracing investigation. *Behav Neurosci* 113**,** 291-302.
Mikulka, P., Vaughan, P., & Hughes, J. (1981). Lithium chloride-produced prey aversion in the toad (Bufo americanus). *Behavioral and neural biology* 33, 220-229.
Nachman, M. (1970). Learned taste and temperature aversions due to lithium chloride sickness after temporal delays. *J Comp Physiol Psychol* 73, 20-30.

Nakamura, K., & Morrison, S.F. (2011). Central efferent pathways for cold-defensive and febrile shivering. *J Physiol* 589, 3641-58.
Nakayama, D., Iwata, H., Teshirogi, C., Ikegaya, Y., Matsuki, N. & Nomura, H. (2015). Long-delayed expression of the immediate early gene Arc/Arg3.1 refines neuronal circuits to perpetuate fear memory. *J Neurosci* 35**,** 819-30.
Pape, H.C., & Pare, D. (2010) Plastic synaptic networks of the amygdala for the acquisition, expression, and extinction of conditioned fear. *Physiol Rev* 90, 419-63.
Paradis, S., & Cabanac, M. (2004). Flavor aversion learning induced by lithium chloride in reptiles but not in amphibians. *Behavioural processes* 67, 11-18.
Plath, N., Ohana, O., Dammermann, B., Errington, M. L., Schmitz, D., Gross, C., Mao, X., Engelsberg, A., Mahlke, C., Welzl, H., et al. (2006). Arc/Arg3.1 is essential for the consolidation of synaptic plasticity and memories. *Neuron* 52**,** 437-44.
Ploski, J. E., Pierre, V. J., Smucny, J., Park, K., Monsey, M. S., Overeem, K. A. & Schafe, G. E. (2008). The activity-regulated cytoskeletal-associated protein (Arc/Arg3.1) is required for memory consolidation of pavlovian fear conditioning in the lateral amygdala. *J Neurosci* 28**,** 12383-95.
Reilly, S. (1999). The parabrachial nucleus and conditioned taste aversion. *Brain Res Bull* 48**,** 239-54.
Reilly, S. (2009). *Central gustatory system lesions and conditioned taste aversion,* New York, NY, Oxford University Press, 309-27.
Reilly, S. & Bornovalova, M. A. (2005). Conditioned taste aversion and amygdala lesions in the rat: a critical review. *Neurosci Biobehav Rev* 29**,** 1067-88.
Rescorla, R. A. (1988). Pavlovian conditioning. It's not what you think it is. *Am Psychol* 43**,** 151-60.
Resendez, S. L., Jennings, J. H., Ung, R. L., Namboodiri, V. M., Zhou, Z. C., Otis, J. M., Nomura, H., Mchenry, J. A., Kosyk, O. & Stuber, G. D. (2016). Visualization of cortical, subcortical and deep brain neural circuit dynamics during naturalistic mammalian behavior with head-mounted microscopes and chronically implanted lenses. *Nat Protoc* 11**,** 566-97.
Roman, C., Nebieridze, N., Sastre, A. & Reilly, S. (2006). Effects of lesions of the bed nucleus of the stria terminalis, lateral hypothalamus, or insular cortex on conditioned taste aversion and conditioned odor aversion. *Behav Neurosci* 120**,** 1257-67.
Roman, C. W., Derkach, V. A. & Palmiter, R. D. (2016). Genetically and functionally defined NTS to PBN brain circuits mediating anorexia. *Nat Commun* 7**,** 11905.
Rosenberg, T., Elkobi, A., Dieterich, D.C., & Rosenblum, K. (2016). NMDAR-dependent proteasome activity in the gustatory cortex is necessary for conditioned taste aversion. *Neurobiology of learning and memory* 130, 7-16.
Sah, P., Westbrook, R. F. & Luthi, A. (2008). Fear conditioning and long-term potentiation in the amygdala: what really is the connection? *Ann N Y Acad Sci* 1129**,** 88-95.
Sanford, C.A., Soden, M.E., Baird, M.A., Miller, S.M., Schulkin, J., Palmiter, R.D., Clark, M. & Zweifel, L.S. (2016). A central amygdala CRF circuit facilitates learning about weak threats. *Neuron* 93, 164-78.
Sclafani, A., & Vigorito, M. (1987). Effects of SOA and saccharin adulteration on Polycose preference in rats. *Neuroscience and biobehavioral reviews* 11, 163-168.
Spector, A. C. (2009). *Central gustatory system and ingestive behavior,* Burlington, MA, Academic Press, 685-89.
Spector, A. C., Norgren, R. & Grill, H. J. (1992). Parabrachial gustatory lesions impair taste aversion learning in rats. *Behav Neurosci* 106**,** 147-61.
St Andre, J., Albanos, K., & Reilly, S. (2007). C-fos expression in the rat brain following lithium chloride-induced illness. *Brain research* 1135, 122-128.

Steward, O. & Worley, P. F. (2001). Selective targeting of newly synthesized Arc mRNA to active synapses requires NMDA receptor activation. *Neuron* 30**,** 227-40.

Swank, M. W. & Bernstein, I. L. (1994). c-Fos induction in response to a conditioned stimulus after single trial taste aversion learning. *Brain Res* 636**,** 202-8.

Terk, M.P., & Green, L. (1980). Taste aversion learning in the bat, Carollia perspicillata. *Behavioral and neural biology* 28, 236-242.

Terrick, T.D., Mumme, R.L., & Burghardt, G.M. (1995). Aposematic coloration enhances chemosensory recognition of noxious prey in the garter snake Thamnophis radix. *Anim Behav* 49, 857-866.

Tokita, K., Inoue, T., & Boughter, J.D. (2009) Afferent connections of the parabrachial nucleus in C57BL/6J mice. *Neuroscience* 161, 475-88.

Tokita, K., Shimura, T., Nakamura, S., Inoue, T. & Yamamoto, T. (2007). Involvement of forebrain in parabrachial neuronal activation induced by aversively conditioned taste stimuli in the rat. *Brain Res* 1141**,** 188-96.

Tsien, J. Z., Huerta, P. T. & Tonegawa, S. (1996). The essential role of hippocampal CA1 NMDA receptor-dependent synaptic plasticity in spatial memory. *Cell* 87**,** 1327-38.

Vardy, E., Robinson, J. E., Li, C., Olsen, R. H. J., Diberto, J. F., Giguere, P. M., Sassano, F. M., Huang, X. P., Zhu, H., Urban, D. J., et al. (2015). A New DREADD Facilitates the Multiplexed Chemogenetic Interrogation of Behavior. *Neuron* 86**,** 936-946.

Ward-Fear, G., Thomas, J., Webb, J.K., Pearson, D.J., & Shine, R. (2016). Eliciting conditioned taste aversion in lizards: Live toxic prey are more effective than scent and taste cues alone. *Integrative zoology* 12, 112-20.

Wickersham, I.R., Lyon, D.C., Barnard, R.J., Mori, T., Finke, S., Conzelmann, K.K., Young, J.A., & Callaway, E.M. (2007) Monosynaptic restriction of transsynpatic tracing from single, genetically targeted neurons. *Neuron* 53, 639-47.

Wilcoxon, H.C., Dragoin, W.B., and Kral, P.A. (1971). Illness-induced aversions in rat and quail: relative salience of visual and gustatory cues. Science *171*, 826-828.

Yamamoto, T., Fujimoto, Y., Shimura, T. & Sakai, N. (1995). Conditioned taste aversion in rats with excitotoxic brain lesions. *Neurosci Res* 22**,** 31-49.

Yamamoto, T., Shimura, T., Sako, N., Azuma, S., Bai, W.Z., & Wakisaka, S. (1992). C-fos expression in the rat brain after intraperitoneal injection of lithium chloride. *Neuroreport* 3, 1049-1052.

Yamamoto, T. & Ueji, K. (2011). Brain mechanisms of flavor learning. *Front Syst Neurosci* 5**,** 76.

Ye, J., & Veinante, P. (2019) Cell-type specific parallel circuits in the bed nucleus of the stria terminalis and central nucleus of the amygdala of the mouse. *Brain Struct Funct* 224, 1067-95.

Yoshihara, Y. (2002) Visualizing selective neural pathways with WGA transgene. Neurosci Res 44, 133-40.

Yu, K., Ahrens, S., Zhang, X., Schiff, H., Ramakrishnan, C., Fenno, L., Deisseroth, K., Zhao, F., Luo, M. H., Gong, L., et al. (2017). The central amygdala controls learning in the lateral amygdala. *Nat Neurosci* 20**,** 1680-1685.

Zhou, P., Resendez, S. L., Rodriguez-Romaguera, J., Jimenez, J. C., Neufeld, S. Q., Giovannucci, A., Friedrich, J., Pnevmatikakis, E. A., Stuber, G. D., Hen, R., et al. (2018). Efficient and accurate extraction of in vivo calcium signals from microendoscopic video data. *Elife* 7.

Zirlinger, M., Kreiman, G., & Anderson, D.J. (2001) Amygdala-enriched genes identified by microarray technology are restrcited to specific amygdaloid subnuclei. *Proc Natl Acad Sci U S A* 98, 5270-5.